



FCTUC FACULDADE DE CIÊNCIAS
E TECNOLOGIA
UNIVERSIDADE DE COIMBRA

DEPARTAMENTO DE ENGENHARIA
MECÂNICA

Tribological Behaviour against Ti6Al4V of Ti- Based Coatings for WC-Co Cutting Tools

Submitted in Partial Fulfilment of the Requirements for the Degree of Master in
Materials Engineering

Author

Dicky Januarizky Silitonga

Advisors

Professor Bruno Trindade

Engineer Renato Monteiro

Jury

President Professor Doutor **Albano Cavaleiro**
Professor at Universidade de Coimbra

Vowel Engineer **João Paulo Dias**
Researcher at Instituto Pedro Nunes

Advisor Engineer **Renato Monteiro**
Researcher at Instituto Pedro Nunes

In the framework of Joint European Master in Tribology of Surfaces and Interfaces



joint european master
in tribology
of surfaces and interfaces
Ljubljana • Leeds • Coimbra • Luleå

Coimbra, July, 2015

ACKNOWLEDGEMENTS

This thesis could not have been finished without the continuous, valuable guidance and advice of my supervisor Renato Monteiro, Professor Albano Cavaleiro and Professor Bruno Trindade. The author would also like to acknowledge the help and support of Dr. Manuel Evaristo as well as other people in the Instituto Pedro Nunes and Department of Mechanical Engineering, University of Coimbra.

Abstract

Titanium alloys are well known as difficult-to-machine materials due to their chemical affinity, low thermal conductivity and low modulus of elasticity, causing premature wear of the tool, compromising the machining quality and increasing costs. Several solutions have been followed to improve the machinability of these alloys: development of new machining techniques, tool geometries and protection of tools' surface with coatings, to yield high productivity, good surface finish of the workpiece and extended tool life. Several Ti-based coatings (WTiN, TiSi(V)N, WTi, TiAlSiCrN, TiAlN and WTiAlN) were tested in this work to evaluate their potential for Ti-alloys machining. The mechanical properties of the different coatings were evaluated by nanoindentation (hardness and Young's modulus) and scratch tests (critical scratch load values). Furthermore, their tribological behaviour was evaluated at room temperature in dry and lubricated conditions on a ball-on-disk equipment, by testing coated balls of 10 mm diameter against Ti6Al4V flat plates. Friction coefficient of coated balls in dry condition was high, as compared to the tests performed with uncoated WC balls. Coatings tested in lubricated condition showed much lower friction coefficient values than their performance under dry condition. In all the tests, adhesion/material transfer of Ti6Al4V to the ball was noticed. Among fifteen tested coatings, the TiSi(V)N coating containing 7 at% Si deposited at 28.31 kW peak power HiPIMS with five V pellets of 10 mm diameter in pure titanium target of 15 cm x 15 cm, and two TiSiAlCrN coatings exhibited the best tribological behaviour.

Keywords: Ti-based coating, Tribology, Titanium machining, WC-Co cutting tools.

Resumo

As ligas de titânio são materiais difíceis de maquinar devido às suas elevada reatividade química, baixa condutividade térmica e baixo módulo de elasticidade. Como resultado, existe um desgaste prematuro da ferramenta de corte, o que compromete a qualidade superficial das peças maquinadas e induz um aumento dos custos de produção. Têm sido equacionadas diversas soluções para melhorar o processo de corte destas ligas, tais como desenvolvimento de novas técnicas de maquinação, e de novas ferramentas de corte revestidas, aumentando assim a produtividade do processo, melhorando o acabamento superficial do material maquinado e aumentando o tempo de vida e rendimento das ferramentas de corte. Nesta tese, diferentes revestimentos à base de Ti (WTiN, TiSi(V)N, WTi, TiAlSiCrN, TiAlN and WTiAlN) foram testados de modo a avaliar o seu potencial como revestimentos de protecção de ferramentas de corte para maquinação de ligas de Ti. As propriedades mecânicas dos revestimentos (dureza e módulo de Young) foram avaliados por ensaios de nano-indentação e ensaios de adesão. Os revestimentos foram ainda testados ao desgaste por pino-disco à temperatura ambiente, a seco e com lubrificação. Para tal foram utilizadas bolas revestidas com 10 mm de diâmetro, contra amostras de Ti6Al4V. Nos testes realizados sem lubrificação, os valores do coeficiente de atrito dos materiais revestidos foram superiores aos obtidos para os materiais não revestidos. Os revestimentos testados em condições de lubrificação apresentaram menores coeficientes de fricção do que quando testados a seco. Em todos os testes ocorreu adesão do material testado (Ti6Al4V) ao contra-corpo. Dos 15 revestimentos estudados, aqueles que apresentaram melhor comportamento tribológico foram o TiSi(V)N com 7% at. Si, depositado por HiPIMS com uma potência de 28.31kW, 5 pastilhas de V com 10 mm de diâmetro sobre um alvo puro de Ti com 15 cm x 15 cm, e dois revestimentos do sistema TiSiAlCrN.

Palavras-chave: Revestimentos à base de Ti, Tribologia, Maquinação de Ti, Ferramentas de corte em WC-Co

CONTENTS

LIST OF FIGURES	xi
LIST OF TABLES	xiv
SYMBOLOLOGY	xv
1. INTRODUCTION	1
1.1. Framework.....	1
1.2. Objectives.....	1
1.3. Thesis structure.....	1
2. INDUSTRIAL PROBLEM.....	3
2.1. The importance of titanium.....	3
2.2. Machining titanium.....	4
2.3. Tool life and wear.....	4
3. STATE OF THE ART	7
3.1. Tool Geometry.....	7
3.2. Machining Operations.....	8
3.3. Cutting tool materials and coatings	10
3.4. Important properties of the coatings for cutting tool	12
4. MATERIALS AND METHODS	15
4.1. Samples	15
4.2. Characterization Methods	16
4.2.1. Nanoindentation test	16
4.2.2. Scratch test	16
4.2.3. Ball on disk test	17
4.2.4. Profilometry, imaging and elemental analysis	19
5. RESULTS AND DISCUSSION.....	20
5.1. Chemical composition of coatings.....	20
5.2. Mechanical properties of coatings	21
5.2.1. Plasticity Index	21
5.2.2. Adhesion and cohesion evaluation of coatings	23
5.3. Tribological performance of coatings	26
5.3.1. WTiN Coating	26
5.3.2. TiSiVN Coatings	29
5.3.3. Coatings from TEandM	32
5.4. Selection of coatings to be deposited on coating tools	34
6. PREPARATORY PROCEDURE FOR FINAL TESTING OF COATED SAMPLE: TOOL GEOMETRY SELECTION.....	37
6.1. Tested geometries	37
6.2. Test methods and conditions	37
6.3. Test results.....	38
6.3.1. Force and moment	38
6.3.2. Wear of cutting edges	39
6.3.3. Surface roughness of finished workpiece	41
6.4. Summary of tool geometry selection	42

7. CONCLUSIONS	43
REFERENCES	44
APPENDIX A – PICTURES OF SCRATCH TEST RESULTS	47
APPENDIX B – 3D PROFILES OF BALLS WEAR SCARS	49
APPENDIX C – RUNNING-IN PERIOD OF FRICTION COEFFICIENT	53

LIST OF FIGURES

Figure 2.1. Cutting tool wear: (a) schematic location of flank and crater wear (b) SEM image of flank, rake and nose wear	5
Figure 2.2. Flank wear of two WC-Co with different grain size (a) 1 μm (b) 0.68 μm	6
Figure 3.1. Examples of various types of drill geometry in the market.....	7
Figure 3.2. Examples of various types of end mill tool geometry in the market	8
Figure 3.3. Effect of feed rate and cutting speed on tool life on Ti6Al4V turning	8
Figure 3.4. The relations of cutting speed on (a) cutting force and feed force; and on (b) tool wear	9
Figure 3.5. (a) Cutting tool life vs cutting speed at various coolant pressure; (b) Wear on tool in different machining condition.....	10
Figure 3.6. (a) effect of Co content on wear (b) effect of grain size on tool life	10
Figure 3.7. Flank wear in milling Ti-6Al-4V with CrN and TiCN coated HSS and uncoated WC-Co tool.....	11
Figure 3.8. TiAlN-PVD coated carbide drill vs uncoated drill: (a) tool life; (b) hole roughness	11
Figure 3.9. Performance of PVD-TiN and CVD-TiCN+Al ₂ O ₃ coated tools on milling Ti-6Al-4V: (a) tool life comparison; (b) flank wear development at 0.15 mm/tooth feed rate	12
Figure 4.1. Nanoindentation instrument.....	16
Figure 4.2. Ball on disk test apparatus at Instituto Pedro Nunes, as used in this work	17
Figure 4.3. Ball on disk test apparatus setup for dry test	18
Figure 4.4. Ball on disk test apparatus setup for lubricated test	18
Figure 5.1. Nanohardness of coatings.....	21
Figure 5.2. Reduced modulus of coatings as measured through nanoindentation	22
Figure 5.3. Plasticity Index.....	23
Figure 5.4. Critical load (10 – 50 N scratch test)	24
Figure 5.5. Scratches of TiSiVN #2.....	24
Figure 5.6. Failure modes on scratches of coatings.....	25
Figure 5.7. WTiN friction coefficient evolution on dry ball-on-disk test.....	27
Figure 5.8. WTiN friction coefficient evolution on lubricated ball-on-disk test.....	27
Figure 5.9. Polynomial fitting of WTiN friction coefficient evolution on lubricated ball-on-disk test	27
Figure 5.10. 3D profilometry of uncoated ball wear scar: (a) dry test; (b) lubricated test ..	28

Figure 5.11. 3D profilometry of WTiN coated ball wear scar: (a) dry test; (b) lubricated test.....	28
Figure 5.12. 3D profile volume calculation of balls wear scar	29
Figure 5.13. Wear track specific wear rate on Ti6Al4V disk, against WTiN coating	29
Figure 5.14. TiSiVN friction coefficient evolution on dry ball-on-disk test	30
Figure 5.15. TiSiVN friction coefficient evolution on lubricated ball-on-disk test.....	30
Figure 5.16 Steady state friction coefficient of TiSiVN samples on ball-on-disk test.....	31
Figure 5.17. 3D profile volume calculation of TiSiVN coated balls wear scar	31
Figure 5.18. Wear track specific wear rate on Ti6Al4V disk, against TiSiVN coatings	32
Figure 5.19. Friction coefficient evolution of TEandM produced coatings on dry ball-on-disk test.....	32
Figure 5.20. Friction coefficient evolution of TEandM produced coatings on lubricated ball-on-disk test	33
Figure 5.21. Steady state friction coefficient of TEandM coatings samples on ball-on-disk test.....	33
Figure 5.22. 3D profile volume calculation of TEandM coated balls' wear scar	34
Figure 5.23. Wear track specific volume of Ti6Al4V disk, against TEandM coatings	34
Figure 5.24. Friction coefficients of selected coatings.....	35
Figure 5.25. Specific wear rate of Ti6Al4V disks against selected coatings.....	35
Figure 5.26. 3D measurements of ball wear scar of selected coatings.....	36
Figure 6.1. Prototypes of milling tools being tested.....	37
Figure 6.2. Kistler 9123C dynamometer	37
Figure 6.3. Force and moment during first phase of test.....	38
Figure 6.4. Force and moment during second phase of test	39
Figure 6.5. Flank wear on prototype E922_10949.....	40
Figure 6.6. Flank wear on prototype E922_10950.....	41
Figure 6.7. Flank wear on prototype E922_10953.....	41
Figure A.1. Scratches of WTiN.....	47
Figure A.2. Scratches of TiSiVN #1	47
Figure A.3. Scratches of TiSiVN #2	47
Figure A.4. Scratches of TiSiVN #3	47
Figure A.5. Scratches of TiSiVN #4	47
Figure A.6. Scratches of TiSiVN #5	48
Figure A.7. Scratches of TiSiVN #6	48
Figure A.8. Scratches of TiSiVN #7	48

Figure A.9. Scratches of TiSiVN #8	48
Figure A.10. Scratches of TEandM #2	48
Figure B.1. Wear scar on uncoated ball: (a) dry test; (b) lubricated test	49
Figure B.2. Wear scar on WTiN ball: (a) dry test; (b) lubricated test	49
Figure B.3. Wear scar on TiSiVN #1 ball: (a) dry test; (b) lubricated test	49
Figure B.4. Wear scar on TiSiVN #2 ball: (a) dry test; (b) lubricated test	50
Figure B.5. Wear scar on TiSiVN #3 ball: (a) dry test; (b) lubricated test	50
Figure B.6. Wear scar on TiSiVN #4 ball: (a) dry test; (b) lubricated test	50
Figure B.7. Wear scar on TiSiVN #5 ball: (a) dry test; (b) lubricated test	51
Figure B.8. Wear scar on TiSiVN #6 ball: (a) dry test; (b) lubricated test	51
Figure B.9. Wear scar on TiSiVN #7 ball: (a) dry test; (b) lubricated test	51
Figure B.10. Wear scar on TiSiVN #8 ball: (a) dry test; (b) lubricated test	51
Figure B.11. Wear scar on TEandM #2 ball: (a) dry test; (b) lubricated test	52
Figure C.1. Running in period of WTiN in dry condition	53
Figure C.2. Running in period of WTiN in lubricated condition	53
Figure C.3. Running in period of TiSiVN in dry condition	53
Figure C.4. Running in period of TiSiVN in lubricated condition	54
Figure C.5. Running in period of TEandM coatings in dry condition	54
Figure C.6. Running in period of TEandM coatings in lubricated condition	54

LIST OF TABLES

Table 2.1. Properties of typical aerospace materials (Al-7075, Ti6Al4V, CFRP).....	3
Table 4.1. Samples description	15
Table 5.1. Chemical composition of coatings	20
Table 5.2. Nanoindentation test results.....	22
Table 5.3. Critical loads from scratch tests.....	23
Table 6.1. Critical loads from scratch tests.....	38
Table 6.2. Surface roughness of finished workpiece resulted by different tool.....	41

SYMBOLOLOGY

a_e	Working engagement
a_p	Depth of cut
CoF	Coefficient of friction
E	Young's modulus
E_r	Reduced modulus
f_n	Feed per revolution
F_z	Force in z-axis direction
H	Hardness
M_z	Moment about z-axis
n	Spindle speed
ν	Poisson's ratio
PI	Plasticity index
R_a	Arithmetic average roughness
R_z	Mean roughness depth (DIN)
V_b	Flank wear
v_c	Cutting speed
v_f	Table feed

1. INTRODUCTION

The title of this thesis is “Tribological Behaviour against Ti6Al4V of Ti-Based Coatings for WC-Co Cutting Tools”, submitted in partial fulfilment of the requirements for the degree of Master in Materials Engineering.

1.1. Framework

This work is a part of a project called Comptitool conducted in the Instituto Pedro Nunes in collaboration with industry. Previous work related to this includes the benchmarking of cutting tools from different manufacturers available in the market to compare and study their performance. Also, there is ongoing study of coatings containing vanadium to induce self-lubrication effect, which is also being tested on this project. All of the works make up a thorough investigation to reveal the performance and characteristics of coated cutting tools to be developed in this project.

1.2. Objectives

In this work, the performance of different coatings deposited on cutting tools is studied. Through series of tests and measurements, each coating is characterized, then some of the outstanding performers are selected for further stages, i.e. deposition on the cutting tools either drills or milling cutters.

Examination on coatings includes the chemical, mechanical and tribological aspects which are in close relation with machining operations. Deeper studies on the coating’s deposition methods, techniques and microstructural analysis were done by other groups in Instituto Pedro Nunes (IPN) and University of Coimbra. As the result of investigation, a picture of how particular coatings behave is to be made available, therefore besides only giving a go or no-go decision for the next stage in this work, some important information can be acquired for other researches and improvements.

The ultimate goal of Comptitool project, which this work is part of, is to develop tools with improved performance for cutting Ti-alloys (mainly Ti6Al4V) and composites material (carbon fiber reinforced plastic, CFRP) as well as their combination (stacks of Ti6Al4V and CFRP) through optimum combination of tool geometry, coatings and machining parameters. This work focuses on performance of the produced coatings against Ti6Al4V, hence tests are associated with that material only. That way, the results of this work will also serve as inputs to the next studies on composite workpiece.

1.3. Thesis structure

This document is presented in chapters that are arranged systematically to relate one with the others to give a clear understanding of the whole work. The chapters divisions are as follows:

1. **Introduction:** provides the overview of this work and the objectives as the ground of the research.
2. **Industrial problems:** discusses the existing conditions in the industries, related to the subjects of studies.
3. **State of the Art:** elaborates current knowledge of the issues and progress on finding the solution to the related problems. Literature, previous works

and other resources are reviewed to provide ideas and considerations for this research.

4. **Materials and methods:** describes samples and methods utilized for conducting the experiments and measurements. Details on the approaches and conditions of the experiments are introduced in order to make complete understanding of the results.
5. **Results and discussion:** reveals and explains the observed phenomena and other experimental outcomes, correlated with the theories and previous relevant works of others.
6. **Preparatory procedures for final testing:** presents the selection procedures of tools that are, in the next stage of this project, to be deposited with selected coatings investigated in this work.
7. **Conclusions:** summarizes the obtained results of this study in relation to the stated objectives, with some comments for potential future works.
8. **References:** lists all literature consulted and referred in this work.

2. INDUSTRIAL PROBLEM

Machining of titanium has been practiced extensively in many industries particularly in, but not limited to, aerospace sectors. The selection of tools and machining conditions are very important aspect in order to achieve maximum productivity with minimum cost to produce components that meet the requirements. With the increasing usage of titanium in aerospace industry, there are potentials to optimize the manufacturing efficiency by improving performance of cutting tools used in machining process.

2.1. The importance of titanium

Along with Al-alloys (such as Al7075), Ti-alloy (Ti6Al4V) and carbon fiber reinforced polymer (CFRP) composite are important materials in aerospace industry nowadays. There are titanium alloys with different compositions but the Ti6Al4V one is the most common type. Besides its corrosion resistance, titanium is superior when compared to aluminum in terms of strength-to-weight property and high temperature performance. Therefore, titanium is usually applied on a component that should bear large amount of load with minimum dimension such as the landing gear and wing-fuselage connections. Also, it is suitable for application in the elevated temperature area such as for engine components.

Composites, mainly CFRPs, is gaining more roles nowadays [1] than it was in the past, commonly for the structures as well as cool sections of the engines to reduce weight. It has better strength-to-weight ratio than aluminum (Table 2.1) hence more proportion of this material in the aerostructure can reduce weight, thus improving fuel economy and increasing payload.

Table 2.1. Properties of Al7075, Ti6Al4V and CFRP (Granta Design Ltd.)

Properties	Al-7075	Ti6Al4V	CFRP
Yield strength (MPa)	359 – 530	827 – 1070	627 – 910
Hardness (HV)	152 – 168	380 – 420	10.8 – 21.5
Density (kg/m ³)	2770 – 2830	4410 – 4450	1540 – 1610
Strength-to-weight ratio (kN.m/kg)	128 – 190	186 – 241	399 – 580
Fracture toughness (MPa.m ^{0.5})	26.6 – 26.8	82 – 100	37.9 – 50.3
Fatigue strength at 10 ⁷ cycles	152 – 168	613 – 638	345 – 592
Thermal conductivity (W/(m°C))	131 – 137	7.1 – 7.3	1.08 – 2.2
Maximum service temperature (°C)	110 – 170	357 – 399	140 – 220
Young's Modulus (GPa)	69 – 76	110 – 177	62.7 – 68.7

Recently, hybrid materials in the form of the stacks of Ti and composite are also introduced in aircraft industry to achieve better strength-to-weight ratio. This kind of

material raises challenge in machining processes because very different properties and behaviour of composite and titanium exist in the same workpiece to be cut with the same tool. Certain machining parameters, tool geometry and material would be suitable in machining titanium but not in composite and vice versa. It would be ideal to have a tool that has a capability of cutting the stack in one go with reasonably high productivity.

2.2. Machining titanium

Machining is an important stage during material processing to create the final shape of the components. Depending on the complexity, machining process may remove up to 90% of material, for instance on an intricate component. For efficiency and productivity, the industry demands high cutting speed as well as good surface finish with lower cost and reduced lead time. However, those expectations have obstacles against titanium workpiece because of its hardness, chemical reactivity and low thermal conductivity. As a comparison, typical maximum drill speed for 12 mm hole on aluminium is around 1000 rpm while on titanium is 150 rpm [1].

Workpiece with high hardness leads to higher cutting forces which then generates more heat that titanium cannot readily dissipate it. Most of the heat generated in cutting area goes to the tool (80%) [2], creating elevated temperature that along with the reactivity of titanium may promote chemical reaction that accelerates wear of cutting tool. This heat generation is also problematic in the case of machining titanium-composite stacks because the high temperature created as the tool cuts titanium makes adverse effect on the adjacent composite layer, causing delamination.

Chatter is also a problem in machining titanium due to its low modulus of elasticity. Titanium demonstrates deflection twice of the carbon steel and as it bounces back, it causes wear on flank and vibration [3]. Vibration affects the surface finish of workpiece and also burdens the spindle bearings.

Tool wear, besides reducing efficiency and productivity, also creates poor surface finish on machined parts [4]. High precision components require tight control on dimensions and roughness. Certain level of tool wear can increase surface roughness of workpiece meanwhile imperfection can lead to a rejection of finished product. Therefore, it is essential to have cutting tool with extended life in terms of the level of wear, not only to reduce lead time but also to maintain machining quality.

2.3. Tool life and wear

The expected cutting tool materials are those having combination of wear resistance and chemical stability at high temperature. When machining titanium, cutting tool is exposed to severe thermal and mechanical conditions that generate high stresses and heat at the cutting edge which affect tool wear rate. The common wear mechanisms on machining titanium are diffusion, abrasion, attrition, chipping and plastic deformation [5]. Those mechanisms cause flank wear, crater wear, chipping and fracture of cutting tool. Figure 2.1(b) shows wear on the flank, nose and rake of a cutting tool. Depending on machining conditions and tool-workpiece material pair, the severity of each mechanism (therefore the caused wear modes) will be different.

Flank wear, as per ISO 8688, is regarded as the criterion of end of tool life, with the typical flank wear (V_b) limit of 300 μm . Some authors also use different values, for instance 150 μm , 200 μm or 500 μm , relevant to the cases of interest. In this work, the end

of tool life criterion is set at $Vb = 200 \mu\text{m}$, which is lower than the typical value in order to keep the research outcomes above standard and at the same time, provide some margin of safety. In addition, the aim of this work is mainly to the aerospace industry where precision is of high importance.

In high speed machining, plastic deformation due to compressive stresses can be a major contributor to tool wear while high temperature that is created during the process may lower the yield strength of material. This extreme conditions occurred on the flank close to the nose causing more rapid wear rate on this area [6]. Materials with low friction coefficient will be beneficial in lowering the forces as well as temperature at the contact area.

Diffusion wear takes place on tool as observed by Arrazola *et al.* [7], who identified carbon content on workpiece material adhered on rake face of cutting tool when turning titanium alloys with cemented carbide tool. It indicates that carbon of the tool had diffused to the workpiece material at the tool-chip interface. At interfacial temperature in excess of 500°C , titanium starts to diffuse into the materials of tool and react with carbon in the tool to form TiC (titanium carbide) on interlayer which then fractured and carried away by the flowing chip. This continuous mechanism of TiC formation, its fracture and removal causes wear on the cutting tool. However, when machining in low speed, there is only minor effect of titanium and carbide reaction. In that case, abrasion is the main mechanism on tool wear during machining titanium with carbide tool [3].

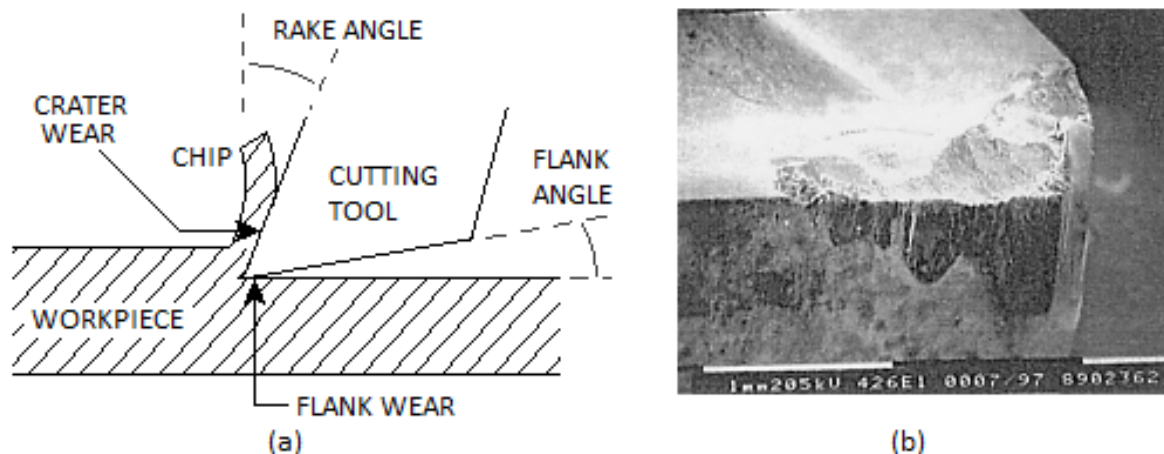


Figure 2.1. Cutting tool wear: (a) schematic location of flank and crater wear (b) SEM image of flank, rake and nose wear [5]

Other findings mentioned that the significance of diffusion and attrition wear on tool flank and rake are different depending on the material of cutting tools. On uncoated cemented carbide and ceramic tools, diffusion wear dominates rake face while attrition creates more wear on the flank face. However, on straight-grade cemented carbide (WC + Co), flank wear also mainly due to diffusion instead of attrition [8]. Che-Haron [6] observed that besides the fact that flank wear increases with the cutting speed and feed rate, wear rate were also different depending on tool material. In Figure 2.2, tool materials are WC-Co with the same composition (94 wt.% WC with 6 wt.% Co binder) yet differ in grain size: $1 \mu\text{m}$ and $0.68 \mu\text{m}$, respectively.

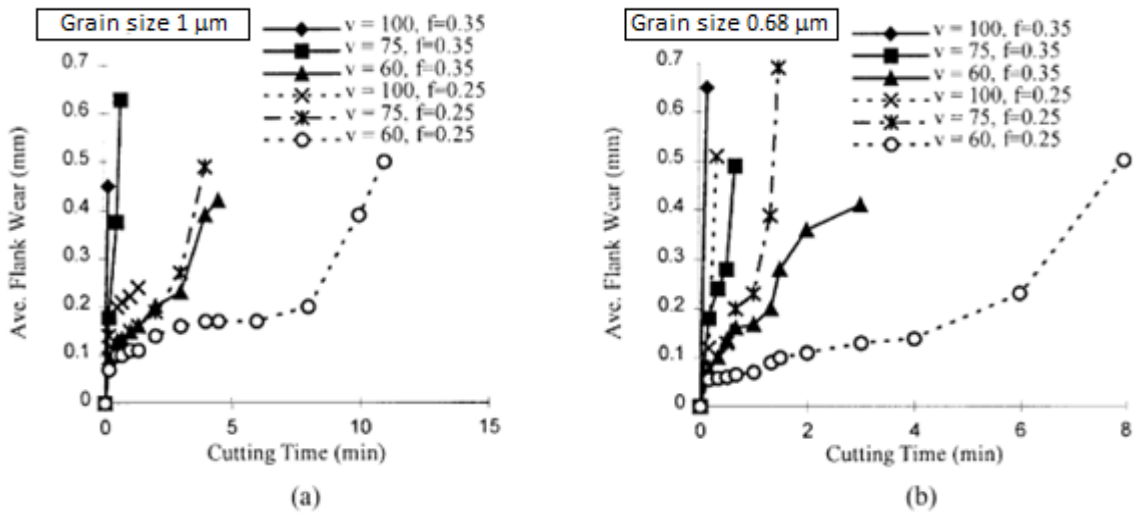


Figure 2.2. Flank wear of two WC-Co with different grain size (a) 1 μm (b) 0.68 μm (v = cutting speed, m/min; f = feed rate, mm/rev) [6]

Niu *et al.* [9] also found that adhesion wear occurred on Ti-alloy/WC-Co tribosystem during dry ball on disk test (WC-Co ball against Ti-alloy disk), indicated by the existence of W element on the worn surface of Ti-alloys according to EDS observation. Titanium has strong reactivity in a tribopair that causes tendency of welding or adhesion onto its counterface [9–12]. This property is attributed to its inability to maintain oxide film on the surface which then causes direct metal to metal contact. It leads to higher friction, chipping on the rake and flank face and the formation of built up edge (BUE) at the tip of cutting edge. These can be problematic as they increase cutting forces, shorten tool life and yield poor surface finish of work material.

3. STATE OF THE ART

Search of the ways to improve efficiency of machining process are still running. Some aspects can be areas of interest, for instance regarding the geometry of cutting tool, optimum machining operations and also cutting tool material and coatings, in order to achieve minimum tool wear and longer tool life. Even though this thesis focuses on the coatings, geometry and machining operations are integral parts of the process, therefore brief discussions on them in this document are considered useful.

3.1. Tool Geometry

The selection of tool geometry can affect machining performance. Some examples of investigated cases of tool geometry approaches to achieve optimum machining result have been published. Geometry of cutting tool such as nose radius, rake angle and clearance/flank angle has influence on cutting forces and stresses because it affects the tool-chip contact area [13]. Komanduri and Reed [14] found that during machining titanium alloy, high flank angle (10° to 15°) and high negative rake angle (-10° to -15°) significantly increased tool life of straight-grade WC-Co tool up to two times. However, the geometry aspect is also being compromised with the machining conditions and tool materials.

Different manufacturers in the market produce tools of different geometries, some of them are shown as examples in the Figure 3.1 and 3.2. The differences may appear in the angles (point angle, helix angle, etc), the number of flutes, cutting edges shape and dimensional measurements. However, the comparison of those tools available in the market to see the effect of geometry alone cannot be obtained only by testing each of those tools on workpiece because each one may have different material composition that becomes another variable determining the performance.

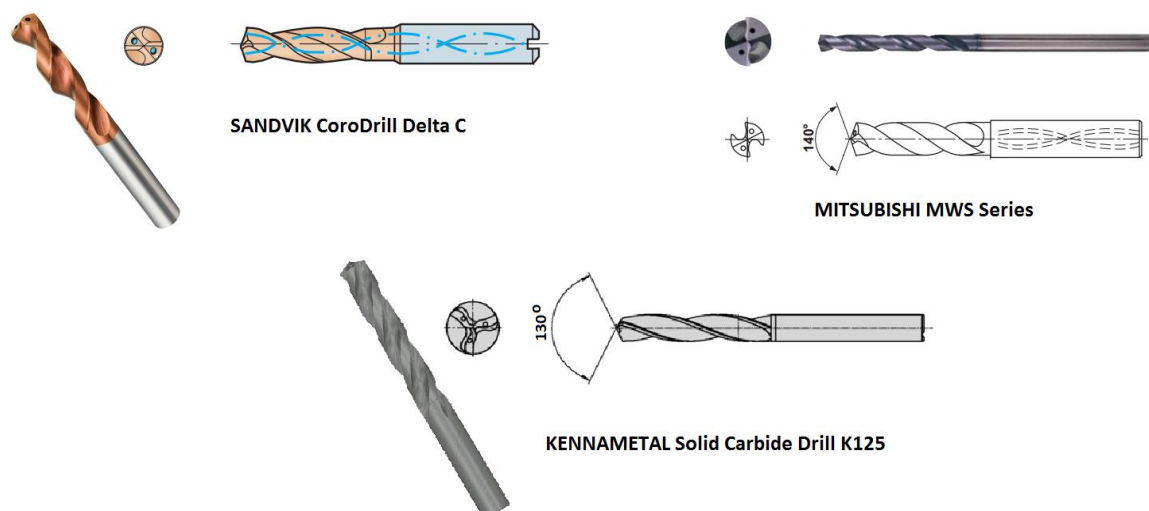


Figure 3.1. Examples of various types of drill geometry in the market

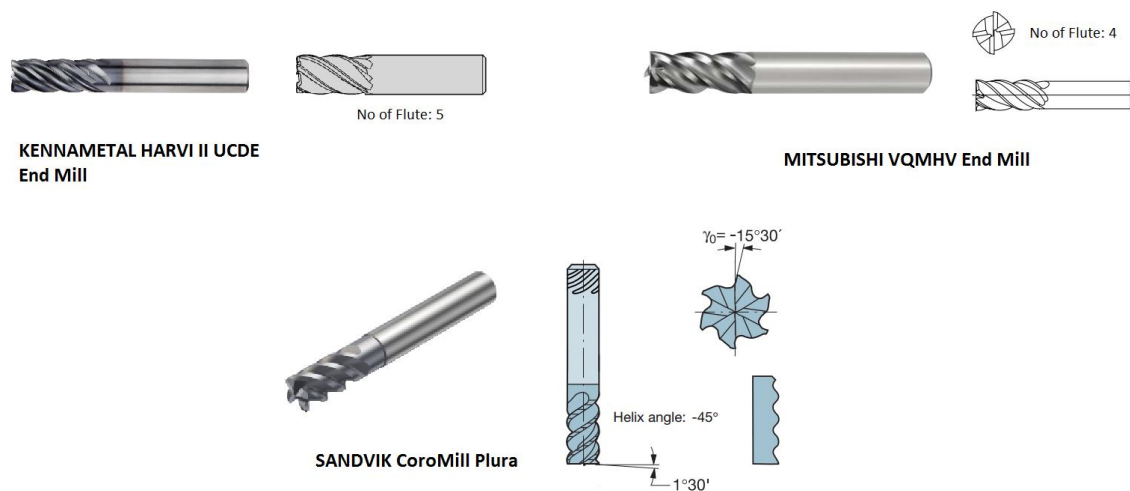


Figure 3.2. Examples of various types of end mill tool geometry in the market

3.2. Machining Operations

Machining conditions such as the setting of speed and feed parameters as well as the existence of coolant or lubricant also have influence on machining product and tool life. Tool life is strongly affected by cutting speed and feed rate. As seen in Figure 3.3 which depicts typical effect of feed and speed to tool life on turning Ti6Al4V with WC tool, reduction in cutting speed can result in significant increase of tool life. Current practice of machining titanium with WC tool is commonly within the cutting speed range of 30 – 100 m/min [11].

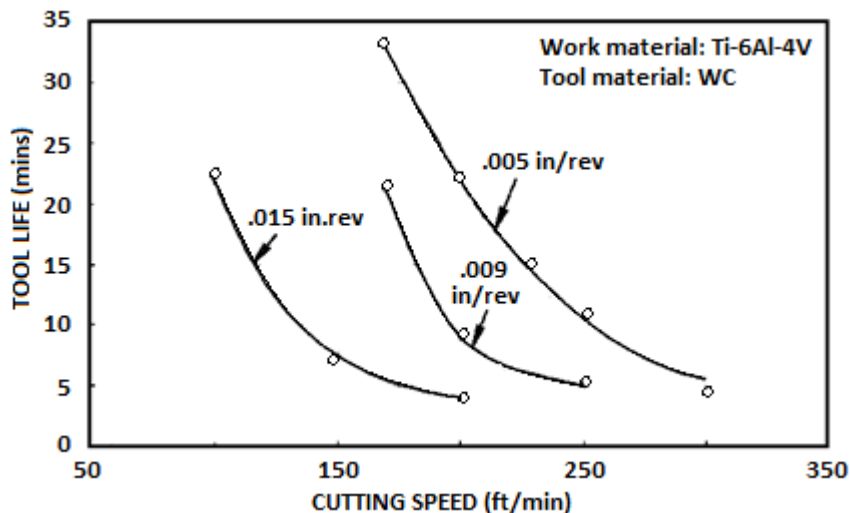


Figure 3.3. Effect of feed rate and cutting speed on tool life on Ti6Al4V turning [8]

When machining titanium alloys, cutting force is reduced at higher cutting speed. This is due to the softening of titanium at elevated temperature due to concentrated heating at cutting area [15]. On the other hand, high cutting speed accelerates cutting tool flank wear due to more intense contact with work material. As illustrated by the work of Arrazola *et al.* [7] in Figure 3.4, when machining two types of Titanium alloys (Ti.555.3 and Ti-6Al-4V), both cutting force and feed force tended to decrease with cutting speed, while the opposite trend occurred on flank wear.

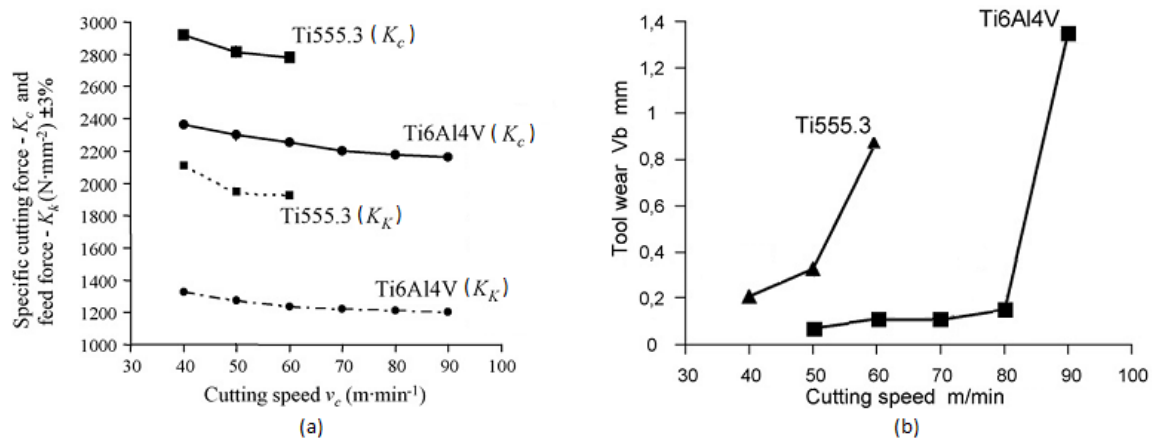


Figure 3.4. The relations of cutting speed on (a) cutting force and feed force; and on (b) tool wear [7]

By recognizing the characteristics of machining results, it is possible to optimize the parameters to achieve particular objectives. For example, in their work Vijay and Khrisnaraj [16] tried to minimize cutting forces and reduce surface roughness of machined material in slot milling operation of Ti-6Al-4V. They found that to reduce cutting force the optimum cutting speed was 40 m/min while to reduce surface roughness it should be 60 m/min.

In machining process that involves generation of high temperature, cooling is important for both workpiece quality and tool life. Da Silva *et al.* [17] discovered that coolant pressure has effects on tool life. They applied higher coolant fluid pressure and reported very significant improvement on tool life up to 21 times compared to conventional cooling fluid supply, when cutting Ti6Al4V using PCD (Polycrystalline Diamond) as shown in Figure 3.5(a). The major difference of tool life as depicted in that chart is obvious in low speed while as the cutting speed increases the difference gets narrower.

Cooling fluid can be introduced by pouring or spraying from the outside (external cooling) and by channeling the fluid through the tool to the tip (internal cooling). Internal cooling is more effective in delivering the coolant to the location where intense heat generating interaction of tool and workpiece occurs. Drilling tools in Figure 3.1 features a cooling channel that facilitates internal cooling. The same type and geometry of cutting tool may have variants of tools with and without cooling channel depending on the needs and suitability to the machine.

Internal cooling creates lower drilling temperature than external cooling does. A study on aluminium drilling by Bagci and Ozelik [18] reported a decrease of temperature up to around 40% on drilling with internal cooling compared to external cooling operation with the same machining parameters. In addition, internal drilling assists chips removal process as the coolant pushes the chips outward while evacuating the drilled hole through the flutes.

However, the use of coolant fluid has also negative issues related to environmental unfriendliness, machining costs due to coolant consumption, industrial laws and regulations as well as the cleanliness of workplace. Based on those considerations, dry machining are preferable whenever possible, but because it generally wears out the tool rapidly, other methods like minimum quantity lubricant and cryogenic machining are promoted in order to minimize or eliminate the need of cutting fluid. The effect of

machining conditions on the cutting tool life is illustrated in Figure 3.5(b), where cryogenic machining demonstrates excellent performance [19].

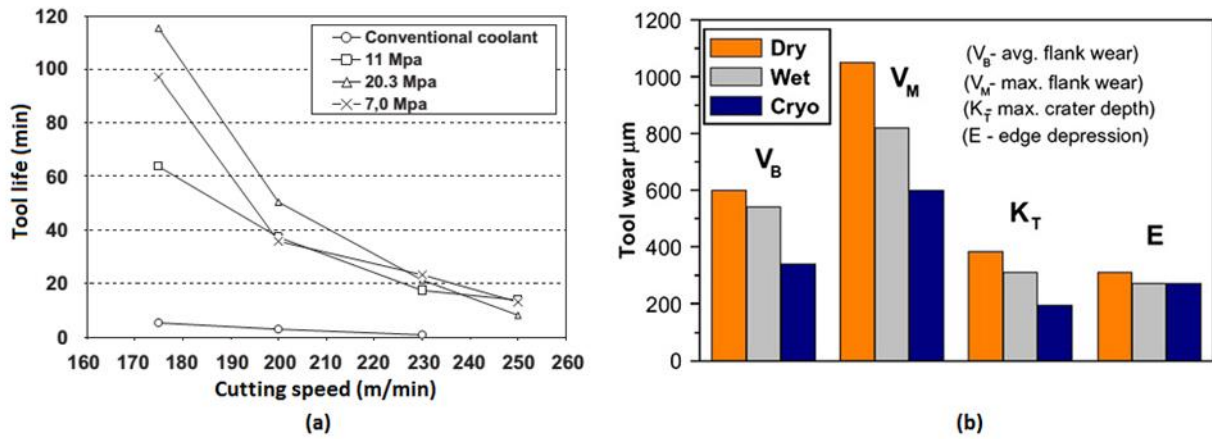


Figure 3.5. (a) Cutting tool life vs cutting speed at various coolant pressure [17]; (b) Wear on tool in different machining condition [19]

3.3. Cutting tool materials and coatings

Current progress on the improvement of tool materials and coatings is the most important subject in this thesis. Studies on the cutting tool materials and coatings for optimum performance on machining titanium and composite have been extensively carried out. For titanium alloys turning and milling, some authors suggest that straight grade uncoated WC-Co tool is more recommended over titanium nitride (TiN) or carbonitride (TiCN) coated tool due to high reactivity of titanium that may create chemical reactions with different titanium components in the tool [20]. However, the developments of coatings are still potential, by looking for solutions to avoid the adverse effects of coating itself.

In the case of the use of WC-Co tool, Co content and WC grain size play important role in relation to tool wear as reported by several authors [5,14]. Figure 3.6 presents the effect of WC-Co composition and grain size on tool wear and life. High amount of cobalt can contribute to wear by plastic deformation [12]. The tool with finer WC grain tends to wear out the flank faster because the solubility of WC in titanium increases as the surface area exposed to solution wear increased [3].

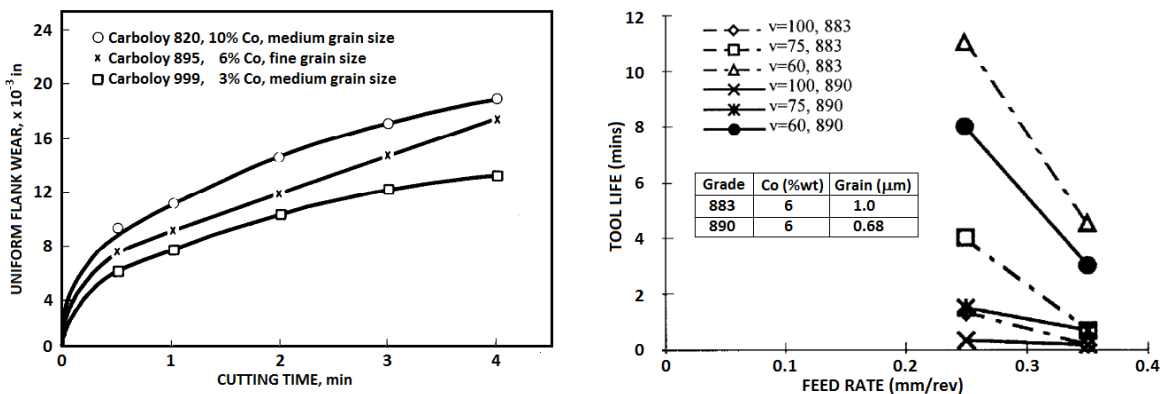


Figure 3.6. (a) effect of Co content on wear [14] (b) effect of grain size on tool life [5]

Turning operation of titanium alloy with straight grade tungsten carbide is usually done with cutting speed of up to about 45 m/min [5]. At higher speed, stresses and temperature will raise such that chemical reaction will occur between titanium and carbon in the tool.

López de Lacalle *et al.* [20] deposited CrN and TiCN on HSS cutting tool and compared the performance with uncoated straight grade tungsten carbide in milling process at cutting speed of 51 m/min (HSS) and 100 m/min (WC). The result was found to be promising as TiCN coated tool went further length to reach the same flank wear as seen in Figure 3.7. Delay on the rapid wear of coated tool was related to the presence of TiCN layer, once it had been exhausted the tool made direct contact with titanium workpiece which boosted up the wear rate. Nevertheless, more in-depth and thorough understanding on the effect of coatings to tool performance is still needed before the coating strategy can be widely applied in industrial practice.

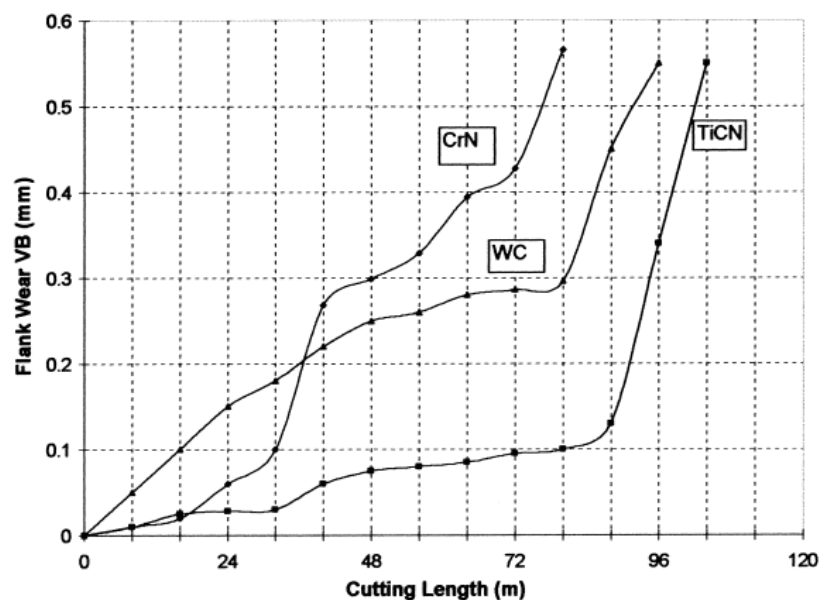


Figure 3.7. Flank wear in milling Ti-6Al-4V with CrN and TiCN coated HSS and uncoated WC-Co tool [20]

In drilling titanium alloy, coated tool also proved better results over uncoated WC-Co in terms of tool life and quality of drilled holes as studied by Sharif and Rahim [21] as illustrated in the graphs in Figure 3.8.

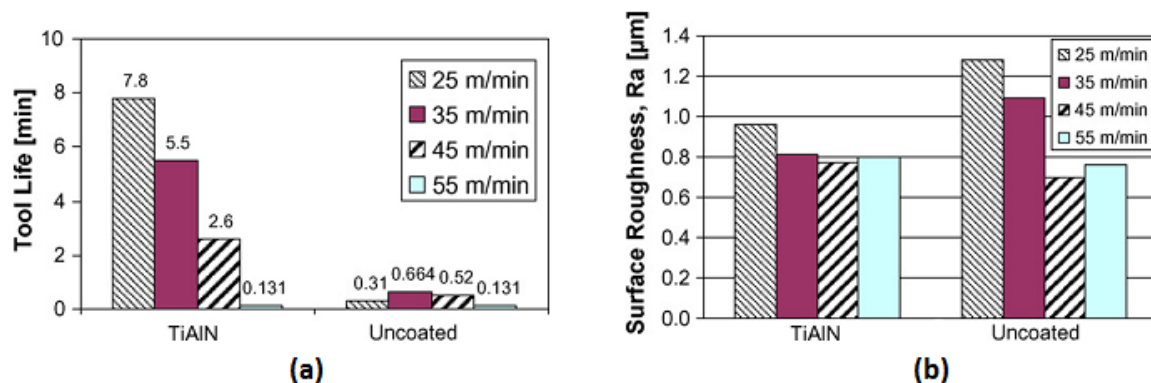


Figure 3.8. TiAlN-PVD coated carbide drill vs uncoated drill: (a) tool life; (b) hole roughness [21]

They observed that 3 μm thick TiAlN – PVD coating on carbide drill made the tool last considerably longer than the uncoated one when they conducted tests on 6 mm diameter, 2-flute drill bits. In addition, the coated drill also produced better surface than the uncoated one. The improvements by coating the tool were more obvious on lower cutting speed. Also, it can be inferred that the surface roughness was related to cutting speed where it decreased as the speed increased, although at even higher speed it increased again, which was most likely due to chattering. These facts indicate that the efforts to make improvement by applying coatings are also connected to other factor, in this case machining parameters.

Coating performance is also different depending on deposition technique because it relates to bonding strength of coating to the substrate. The common coating deposition techniques used for cutting tool are the higher temperature (800 – 1000 °C) CVD and the lower temperature (500 – 600 °C) PVD. Results from the work of Jawaid *et al.* [12] during milling Ti-6Al-4V with cutting inserts coated with TiN by PVD and TiCN+Al₂O₃ by CVD revealed that the CVD deposited tool outperformed the PVD one. Significant difference in tool life was observed on lower cutting speed while at high speed both survived the same short life because of rapid wear that induces chipping and flaking on cutting edge.

In most of tests, as depicted in Figure 3.9(b), flank wear of CVD coated tool developed more gradually which could be due to stronger adhesion produced by CVD technique. The initial wear mechanisms on both tools were coating delamination, galling on rake face and adhesion on the cutting edge. Flank and rake face wear are attributed to attrition and diffusion mechanisms.

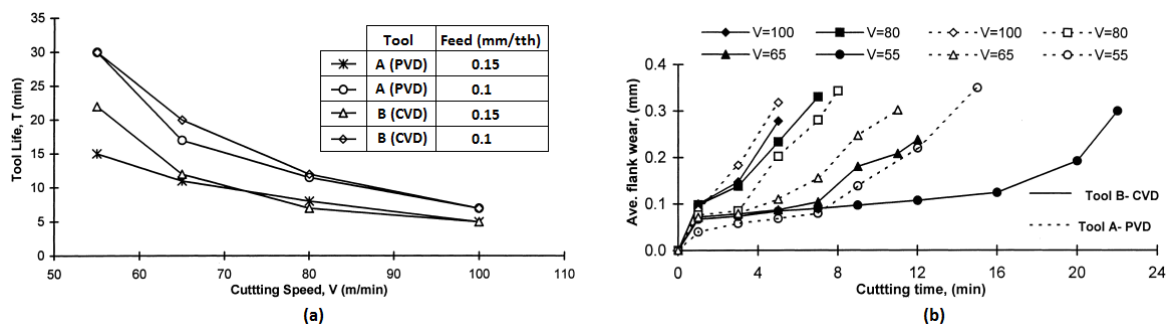


Figure 3.9. Performance of PVD-TiN (tool A) and CVD-TiCN+Al₂O₃ (tool B) coated tools on milling Ti-6Al-4V: (a) tool life comparison; (b) flank wear development at 0.15 mm/tooth feed rate [12]

In the case of composite-metal stacks, problem arises from the difficulty of workpiece to be machined in one-shot, for example during the drilling through the stack of composite-titanium stack. One tool material which works efficiently on metal may not do as good on composite. PCD (Polycrystalline Diamond) is excellent on composite while it is poor on titanium. On the other hand, WC-Co suits titanium but not composite. The expected solution for titanium-composite stacks machining is to have one tool material that performs well on both titanium and composite.

3.4. Important properties of the coatings for cutting tool

The expected coatings should be exceptional in terms of mechanical properties, tribological behavior as well as adhesion strength to its substrate. They are important to ensure the coating to create low friction and low tool wear while effectively cutting the workpiece and being able to withstand high forces without delamination.

Commonly, wear resistance are related to hardness property, however some researchers have suggested the influence of elastic modulus [22]. Coating's elasticity and toughness can also have high importance in the case of abrasion and impact wear. Therefore, for a given hardness (H), lower Young's modulus (E) is better. More ideal situation would be if the E of coating is close to that of the substrate, thus minimizing stresses on the interface of coating-substrate because they deform and relax together without leaving shear stress in the interface and tension within coating.

Accommodating the importance of both H and E , their ratio (H/E or elastic strain to failure) is believed to be the more appropriate means of wear resistance prediction [22,23] instead of examining H only. H/E can be related to dimensionless parameter of plasticity index (PI) obtained from indentation test, which is the ratio of plastic work (W_p) to the total of plastic and elastic work ($W_p + W_e$) during indentation, through the following relation:

$$PI = \frac{W_p}{W_p + W_e} = 1 - x(H/E_r) \quad (\text{Eq. 1.1})$$

With H and E_r (reduced modulus) readily available as the outputs of indentation test, PI can be calculated if the constant x is known. For coatings on WC-Co, Beake *et al.* [23] suggested value of 6.4 for x . Furthermore, they built a list of comparison of PI and tool life on different machining operations of several Ti-based coatings on WC-Co substrates as presented in Table 3.1. They estimated that for WC-Co tool, the optimum PI of coating at room temperature was 0.53 for operations involving cyclic impact and severe loadings such as end milling and drilling. Less value would show lower performance on those operations. On the other hand, lower PI of 0.46 was estimated as the optimum value for continuous cutting as in turning operation.

Table 3.1. PI and machining performance of several coatings on WC-Co substrate

Coatings	PI	Longer tool life in
None (WC-Co substrate)	0.67 – 0.70	
AlCrN	0.56	End milling vs TiAlN
AlTiN	0.51 – 0.51	End milling vs TiAlN
TiAlCrN	0.49 – 0.51	End milling vs TiAlN
TiAlN	0.48	Turning vs TiAlCrN
Annealed AlTiN	0.45 – 0.46	Turning vs AlTiN
TiCN	0.44	
DLC	0.3	

Although most machining processes of titanium involve continuous supply of lubricant/coolant, dry contact can also occur (at least intermittently). Because titanium is poor in dry tribosystems [10], it is advantageous to have a coating with self-lubrication property that will assist especially during dry contact condition. Oxides of some elements can form a film of low shear resistance that induces self-lubrication effect.

Coatings that incorporate vanadium (V) are proved to have self-lubrication properties by producing lubricious oxide V_2O_5 at high temperature in excess of 500 °C [24–27]. Low friction and wear have been reported on some coatings namely TiSiVN, TiAlVN, (V, Ti)N and TiVN [25–27]. These friction and wear reduction on high temperature are very beneficial because that temperature mentioned before is in accordance with what occurs during titanium machining process. On the other hand, the

tendency of titanium to adhere or transfer onto its counterpart in a tribosystem can cancel the functionality of vanadium. The coating that is supposed to diffuse V to form V-O oxide is covered by the transferred titanium, thus the effective contact in sliding motion is titanium against itself instead of coating. Therefore, this issue requires further investigation in order to determine the suitability of this type of coating against titanium and identify areas for improvement.

4. MATERIALS AND METHODS

4.1. Samples

In this work, fifteen different coatings were tested for characterization of mechanical and tribological properties. Classified into three groups for easiness of comparison and selection, the coatings are:

- 1 WTiN coating
- 8 types of PVD deposited TiSiVN coatings with different sputtering conditions (targets materials and power)
- 6 types of coatings produced by a company (TEandM)

Descriptions and designations of samples used in this document are listed in the following table:

Table 4.1. Samples description

No	Sample ID	Description
1	Uncoated	Uncoated WC-Co
2	WTiN	WTiN
3	TiSiVN #1	TiSiVN, 7% Si, 9 Pellets Vanadium, 28.31 kW
4	TiSiVN #2	TiSiVN, 7% Si, 5 Pellets Vanadium, 28.31 kW
5	TiSiVN #3	TiSiVN, 7% Si, 5 Pellets Vanadium, 109.83 kW
6	TiSiVN #4	TiSiVN, 7% Si, 9 Pellets Vanadium, 109.83 kW
7	TiSiVN #5	TiSiVN, 11% Si, 5 Pellets Vanadium, 28.31 kW
8	TiSiVN #6	TiSiVN, 11% Si, 5 Pellets Vanadium, 68.17 kW
9	TiSiVN #7	TiSiVN, 11% Si, 9 Pellets Vanadium, 68.17 kW
10	TiSiVN #8	TiSiVN, 11% Si, 9 Pellets Vanadium, 28.31 kW
11	TEandM #1	TRIBO
12	TEandM #2	HARD SILK
13	TEandM #3	HARD
14	TEandM #4	HARD SILK II
15	TEandM #5	DI EXTRA
16	TEandM #6	DURALUB

The TiSiVN coatings were deposited at working pressure of 1 Pa with different content of silicon (7 at.% and 11 at.%) using HiPIMS (High Power Impulse Magnetron Sputtering) process at varied peak power (28.31, 68.17 kW and 109.83 kW). Different numbers of pellets of pure vanadium and pure silicon were inserted on 99 % pure titanium target, to get the desired amount of silicon and vanadium content. The size of titanium target was 15 cm x 15 cm and the diameter of pellets was 10 mm.

For ball on disk test, coatings were deposited on WC balls of 10 mm diameter. Also, uncoated WC balls were available for testing to provide comparison to the results of coated balls. The thickness of all coatings were 1 μm . As the counterfaces (disk) for the ball on disk test, Ti6Al4V plates were polished to average roughness, R_a , of 0.1 μm .

Coatings were also deposited on flat plates for the purpose of nanoindentation and scratch test analysis. Thickness of coatings were 1 μm as well. Due to limited time frame of this thesis, out of six coatings supplied by TEandM in the form of balls (for ball on disk test), only one coating was made available on flat sample, i.e. TEandM#2 (HARD SILK). This coating was chosen because it was proved to have better tribological behaviour than

other TEandM coatings, based on ball on disk test. Therefore, only one coating from TEandM (TEandM #2) was tested for mechanical and scratch properties in this work.

4.2. Characterization Methods

4.2.1. Nanoindentation test

This test was carried out to investigate mechanical properties of the coatings. From this test, hardness and modulus of the coatings were obtained.

Nanoindentation test instrument returns hardness, H , and reduced modulus, E_r . The E_r value depends on the Young's modulus of sample and indenter, according to the following relation:

$$\frac{1}{E_r} = \frac{1-\nu^2}{E} + \frac{1-\nu_i^2}{E_i} \quad (\text{Eq. 4.1})$$

Where E_i is the Young's modulus of indenter and E_r is the measured reduced modulus of sample. With diamond indenter, the E_i for the calculation was 1100 GPa and Poisson's ratio for indenter, ν_i was 0.07 while Poisson's ratio of sample, ν , was assumed 0.3. Therefore, Young's modulus of coatings could be calculated using the measured E_r value from the test.

The indenter was of Berkovich type and the depth of indentation was ± 100 nm or one-tenth of the thickness of coatings, narrow enough to avoid the effect of substrate on measurements. Silicon were used as substrates for TiSiVN coatings samples while the other samples (WTiN and coating from TEandM) were deposited on WC-Co substrates. Tests were made at room temperature.

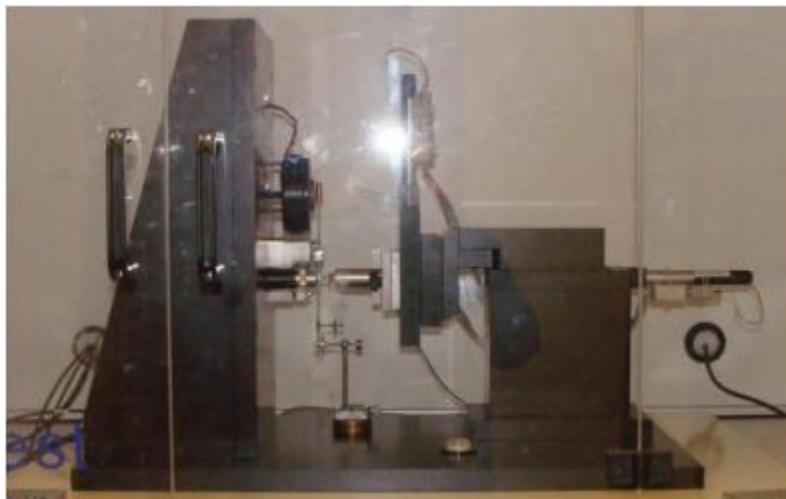


Figure 4.1. Nanoindentation instrument

4.2.2. Scratch test

To study adhesion and cohesion quality of the coating, flat sample of coating deposited on WC substrate were subjected to scratch by diamond Rockwell C indenter of spherical tip with 0.2 mm radius. The loading was 10 N to 50 N with the increment of 10 N/mm and speed of 10 mm/min. Selection of 10 N as initial load was to create visible starting point for distance measurement on the scratch, which instead would be difficult to

find if the loading started from 0 N. The scratches were then observed under light microscope to evaluate the failure modes.

Determination of critical loads was made by measuring the length along the scratches until the defects or failures were found, which was done in the magnified image of scratch. Then, based on that length the load could be calculated because the load increment per unit length was known (10 N/mm).

4.2.3. Ball on disk test

This test was intended to study tribological behavior of coatings on sliding motion against Ti6Al4V, in accordance with the objectives of this work. The outcomes of this test were friction and wear characteristics of coatings.

Ball on disk apparatus used in this work (Figure 4.2) was a rotating disk with speed controller and a lever that pushed a load cell with the tangential force caused by friction of tribosystem. Signal from load cell was fed to computer at every corresponding rotation/cycle of the disk. As the reading from load cell represented friction force and the normal force was known (stacks of disks atop the lever), coefficient of friction at every cycle could be calculated. The number of cycle was set to achieve expected linear distance based on the linear speed and sliding track radius.

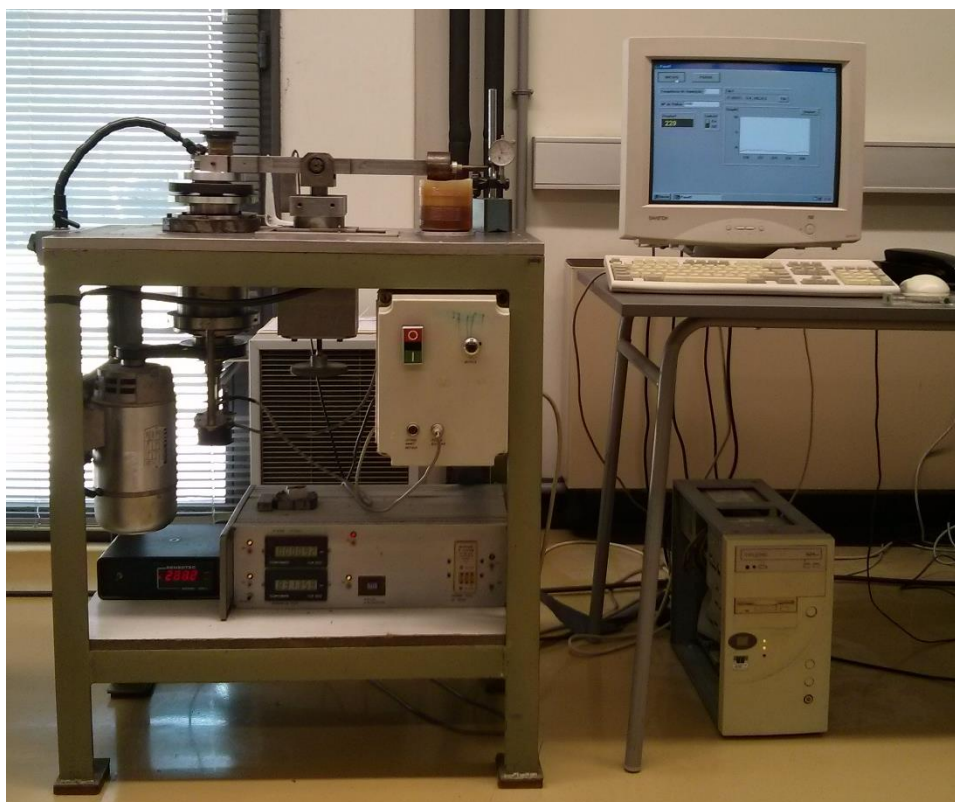


Figure 4.2. Ball on disk test apparatus at Instituto Pedro Nunes, as used in this work

Ball-on-disk tests were conducted in conformance with ASTM G99. The linear speed for all tests in this work was 0.1 m/s and linear distance for dry and lubricated tests were 20 m and 100 m, respectively. Normal load applied was 5N for both dry and lubricated tests. Those parameters were chosen following several preliminary tests which indicated that with higher load and longer distance, the resulted scar was very severe such that the coating was completely removed. Once the coating was removed, the sliding

contact took place was basically between the substrate of ball (WC-Co) against Ti6Al4V, which would mislead the interpretation of the behaviour of coatings. In addition, previous research on WTiN coatings by a group in University of Coimbra and Instituto Pedro Nunes (IPN) was also conducted with the same parameters [28].

The differences in apparatus setup for dry test and lubricated test as seen in Figures 4.3 and 4.4, were only in the presence of liquid container and liquid diverter plate in lubricated test.

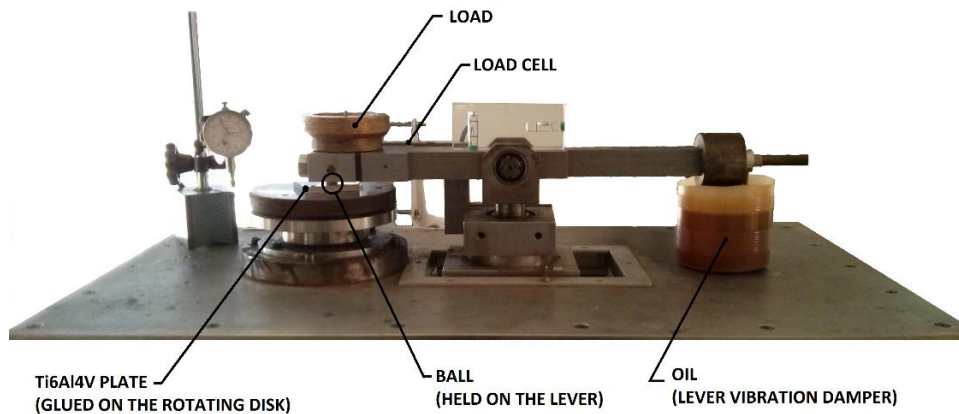


Figure 4.3. Ball on disk test apparatus setup for dry test

Lubricated ball on disk test was carried out with a container in which the Ti6Al4V plate was immersed in cutting fluid (Castrol Cooledge, 5%) up to slightly higher than its surface so the contact with the ball was lubricated. To prevent the liquid from being displaced centrifugally outwards that might leave the center area of container dry and/or spill the lubricant out of the container, a plate was placed near to the periphery of the container, acting as a diverter that redirect the lubricant inwards.

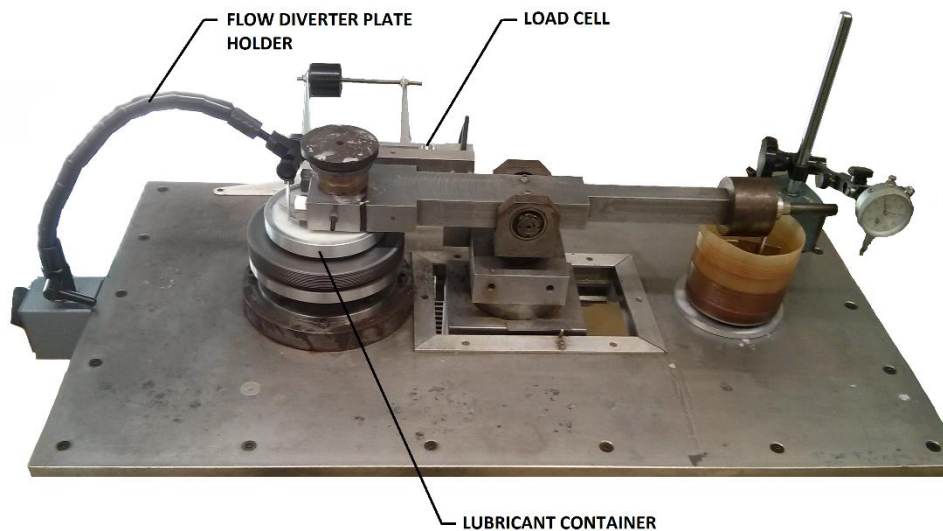


Figure 4.4. Ball on disk test apparatus setup for lubricated test

4.2.4. Profilometry, imaging and elemental analysis

Profile of the surface was measured by 2D profilometer (Mahr Perthometer S4P with Focodyne laser head), to acquire surface roughness, film thickness as well as depth of profile such as in wear track measurement.

A light microscope with 3D measurement capability, Alicona InfiniteFocus, was utilized for analysis of wear scars and scratches. Wear scar measurements were made by taking the profile/measurement of virgin surface first, then the scar was measured after ball on disk test. Using the profile of virgin surface as reference, the instrument calculated the volume above and below the reference. In general, volume above the reference could be presumed as adhesion or material transfer, while that below was considered as wear.

For elemental analysis, a JEOL scanning electron microscope with Oxford Instruments EDS (Energy Dispersive Spectroscopy) detector was employed. Accelerating voltage was set to 20kV to be able to identify heavier elements existed in the samples. This method allowed qualitative analysis on what elements present in the sample and quantitative calculation of relative composition of each component.

5. RESULTS AND DISCUSSION

Most of the results are discussed according to the coatings groups, namely: WTiN coating (only one type), TiSiVN coatings (eight types) and the coatings from TEandM (six types). Afterwards, one or more coatings that show outstanding performance in each group are selected and then deposited on cutting tools in the next stage of this project.

5.1. Chemical composition of coatings

Chemical composition of the coatings was examined with SEM-EDS in area mode. Results are presented in Table 5.1. The coatings contain Ti with different amount of proportion.

Table 5.1. Chemical composition of coatings

Sample	Description/Commercial Name	Composition	
		Elements	Atomic %
WTiN Coating			
WTiN	WTiN	W	39.3
		Ti	27.8
		N	32.9
TiSiVN Coatings			
TiSiVN #1	TiSiVN, 7% Si, 9 Pellets Vanadium, 28.31 kW	Ti	28.0
		Si	6.9
		V	12.0
		N	53.2
TiSiVN #2	TiSiVN, 7% Si, 5 Pellets Vanadium, 28.31 kW	Ti	32.7
		Si	7.1
		V	6.4
		N	53.8
TiSiVN #3	TiSiVN, 7% Si, 5 Pellets Vanadium, 109.83 kW	Ti	32.9
		Si	7.1
		V	5.8
		N	54.2
TiSiVN #4	TiSiVN, 7% Si, 9 Pellets Vanadium, 109.83 kW	Ti	27.5
		Si	6.8
		V	12.1
		N	53.6
TiSiVN #5	TiSiVN, 11% Si, 5 Pellets Vanadium, 28.31 kW	Ti	27.5
		Si	11.3
		V	6.2
		N	55.0
TiSiVN #6	TiSiVN, 11% Si, 5 Pellets Vanadium, 68.17 kW	Ti	25.9
		Si	12.9
		V	5.8
		N	55.3

TiSiVN #7	TiSiVN, 11% Si, 9 Pellets Vanadium, 68.17 kW	Ti	23.7
		Si	11.0
		V	10.4
		N	54.9
TiSiVN #8	TiSiVN, 11% Si, 9 Pellets Vanadium, 28.31 kW	Ti	21.5
		Si	14.4
		V	10.3
		N	53.9
TEandM Coatings			
TEandM #1	TRIBO	Ti	30.1
		Co	63.5
		W	6.5
TEandM #2	HARD SILK	N	1.5
		Al	4.0
		Si	35.7
		Ti	46.5
		Cr	12.3
TEandM #3	HARD	N	39.1
		Al	29.7
		Ti	31.3
TEandM #4	HARD SILK II	N	2.0
		Al	3.6
		Si	25.3
		Ti	55.5
		Cr	13.7
TEandM #5	DIEXTRA	Cr	98.7
		W	1.3
TEandM #6	DURALUB	N	23.4
		Al	4.1
		Ti	56.7
		W	15.8

5.2. Mechanical properties of coatings

5.2.1. Plasticity Index

WTiN has higher value than all of the tested coatings in terms of both hardness and reduced Young's modulus. A significant difference can be noticed on its reduced Young's modulus, while its hardness is close to that of the others.

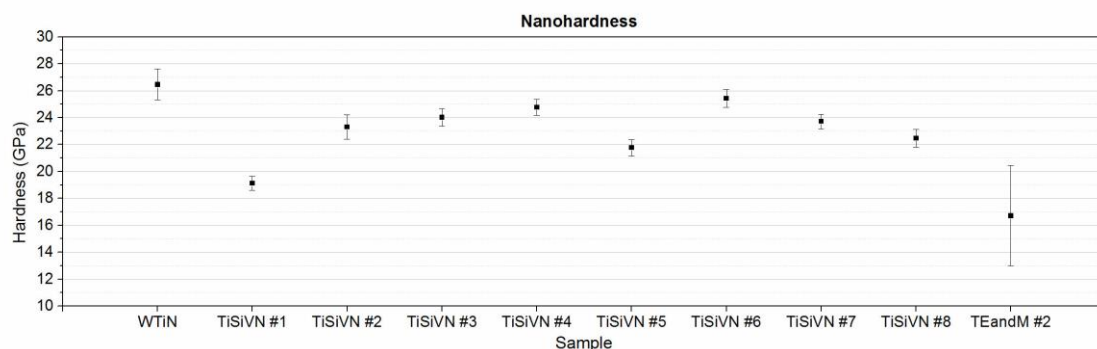


Figure 5.1. Nanohardness of coatings

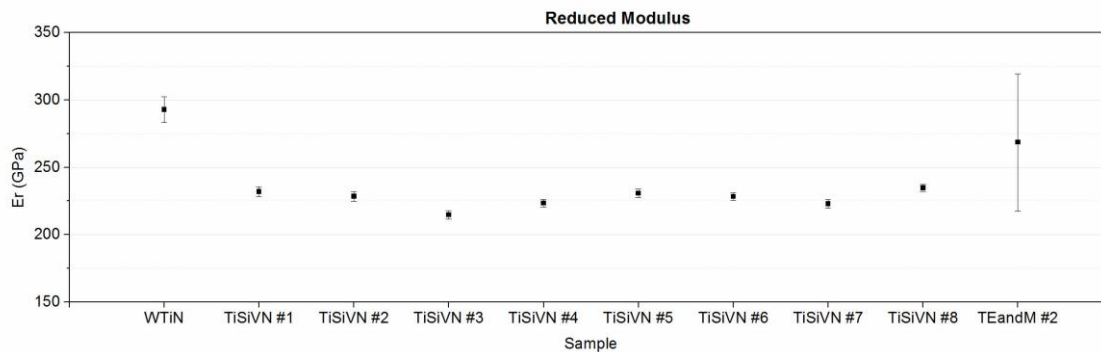


Figure 5.2. Reduced modulus of coatings as measured through nanoindentation

Nanoindentation results, as seen in Figure 5.1 and 5.2, show that the measurement of TEandM #2 had wide deviation (20% to 25% error). This was due to its surface roughness because this coating was deposited on an unprepared/unpolished substrate, whereas the others were deposited on mirror finished substrates.

To predict wear performance of coatings, plasticity index (PI) was used. With nanoindentation test results giving the value of H and E_r , PI was then calculated by recalling Eq. 1.1:

$$PI = 1 - x(H/E_r) \quad (\text{Eq. 1.1})$$

Here the constant x value was 6.4, as suggested by Beake *et al.* [23]. As stated earlier, they found that the optimum PI at room temperature was 0.53 for coatings used for milling/drilling application and 0.46 for turning.

Table 5.2. Nanoindentation test results

Sample	H (GPa)	E_r (GPa)	E (GPa)	PI	PI Rank Within Group
WTiN	26.5 ± 1.2	293 ± 10	362 ± 30	0.42	-
TiSiVN #1	19.1 ± 0.5	232 ± 4	267 ± 10	0.47	1
TiSiVN #2	23.3 ± 0.9	228 ± 4	262 ± 10	0.35	4
TiSiVN #3	24.0 ± 0.6	215 ± 3	242 ± 8	0.28	8
TiSiVN #4	24.8 ± 0.6	223 ± 3	254 ± 7	0.29	7
TiSiVN #5	21.8 ± 0.6	231 ± 3	265 ± 8	0.40	2
TiSiVN #6	25.4 ± 0.7	228 ± 3	262 ± 8	0.29	6
TiSiVN #7	23.7 ± 0.5	223 ± 3	254 ± 9	0.32	5
TiSiVN #8	22.5 ± 0.6	235 ± 3	271 ± 7	0.39	3
TEandM #2	16.7 ± 3.7	268 ± 51	322 ± 154	0.60	-

Nanoindentation results in Table 5.2 indicate that among all of the TiSiVN coatings, TiSiVN #1 has the highest PI , which is also higher than WTiN. However, all TiSiVN coatings have lower PI than the optimum value for milling and only one meets the suggested optimum PI value for turning (#1). With this situation, selection within the group of TiSiVN coatings is based on the rank of higher PI value. Nevertheless, this is not the absolute criterion to select the coating because other characteristics such as coating adhesion to the substrate and tribological performance against workpiece (Ti6Al4V) also

have important roles. In contrast to the other tested coatings, TEandM #2 coating showed high PI with its low hardness and considerably high modulus. However, it should be borne in mind that measurement error of this TEandM #2 coating was high, therefore the actual value might be appreciably higher or lower than that showed in Table 5.2 and Figure 5.3.

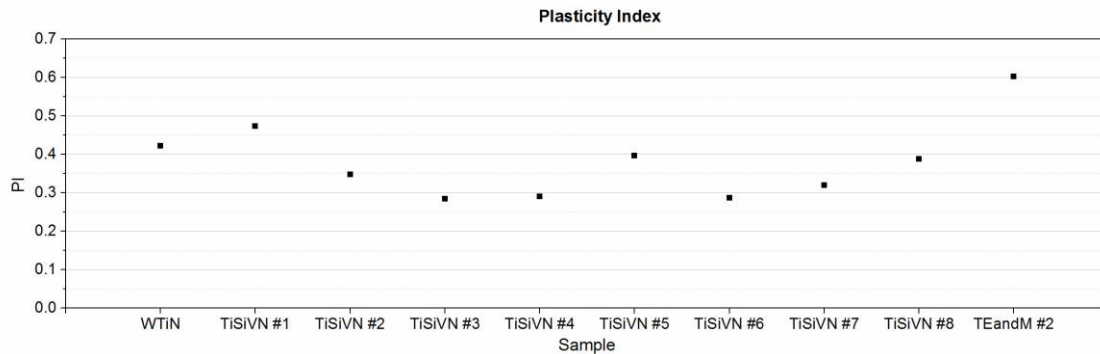


Figure 5.3. Plasticity Index

5.2.2. Adhesion and cohesion evaluation of coatings

Scratch test results are presented in Table 5.3 and Figure 5.4 as three critical loads: L_{c1} (load at the initiation of failure), L_{c2} (load when the coating undergoes consistently substantial damage) and L_{c3} (load at complete delamination/coating peel off).

Within the testing load range (10 – 50 N) most of the coatings withstood complete delamination, except TiSiVN #4 where complete exposure of substrate occurred at 43 N. TiSiVN #2 outperformed all the coatings that it did not show any noticeable failure at the observation magnifications (500x) where failures started to be clearly visible on other coatings.

Table 5.3. Critical loads from scratch tests

Sample	L_{c1} (N)	L_{c2} (N)	L_{c3} (N)
WTiN	25.3	29.87	-
TiSiVN #1	36.7	42.4	-
TiSiVN #2	30.9	-	-
TiSiVN #3	25.3	31.0	-
TiSiVN #4	16.6	26.1	43.0
TiSiVN #5	41.5	46.5	-
TiSiVN #6	32.0	35.4	-
TiSiVN #7	39.3	46.4	-
TiSiVN #8	34.0	42.0	-
TEandM #2	40.1	44.3	-

To compare the performance of coatings, L_{c2} is taken as reference because it is the point where continuous failure occurs, therefore it can be more confidently referred as the failure region. The very first failure that spotted, L_{c1} , may only be a small defect on sample that does not represent the true characteristic of sample. However, if the mark of failure is clear and convincing, L_{c1} can be important to see how the failure initiates and propagates until it forms a substantial failure. The L_{c3} cannot be the basis of comparison in this work because only one coating reached L_{c3} during the test.

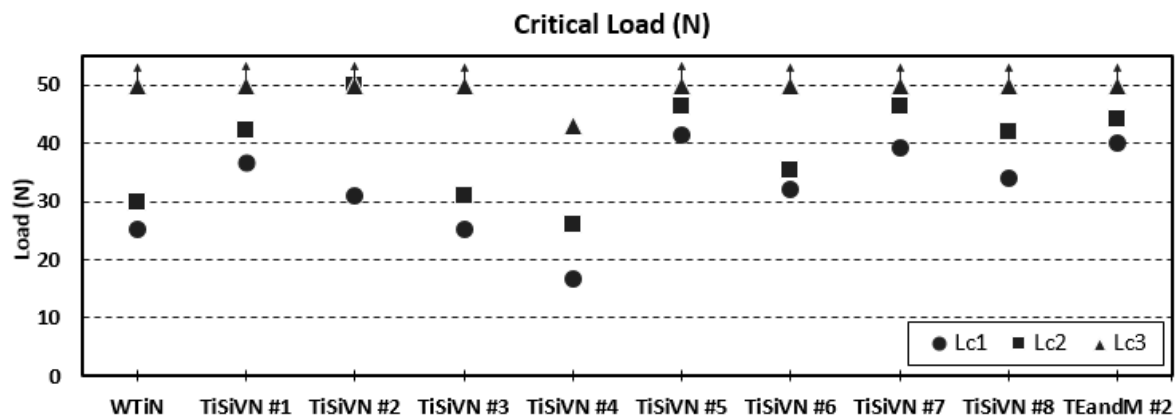


Figure 5.4. Critical load (10 – 50 N scratch test)

In TiSiVN #2, there was no continuous failure observed, therefore L_{c2} was not achieved within loading range (10 N – 50 N). In addition, the small areas of coating removal, which were then selected as L_{c1} , were found near to or at the spots of what looked like flaws on the surface of coating (Figure 5.5). Thus, these failures were probably related to local defect of the sample.

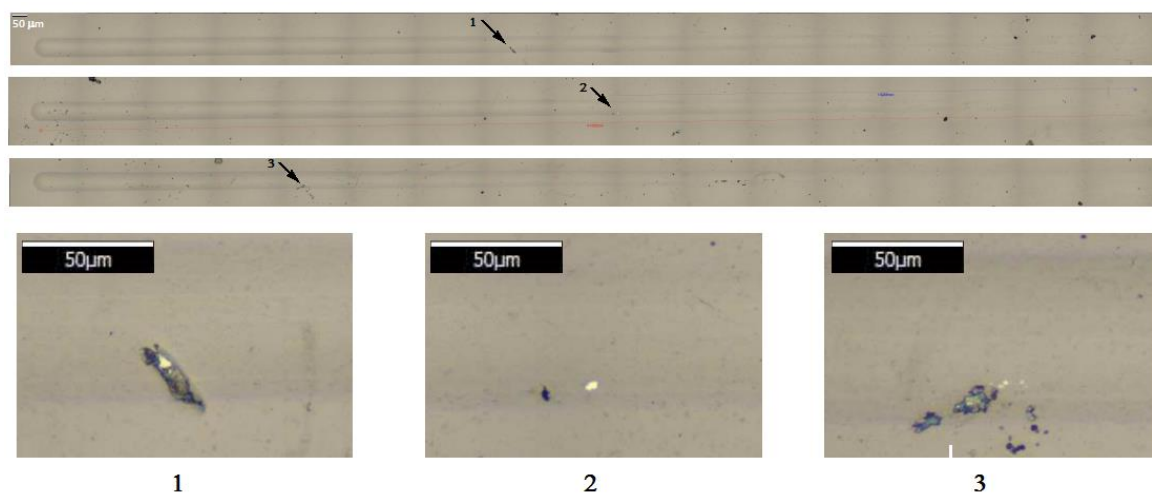


Figure 5.5. Scratches of TiSiVN #2: zoomed-in images of of each location of L_{c1} on 3 different scratches; there is no other failure afterwards

The failure mode occurred on WTiN coating as shown in Figure 5.6 is a compressive or wedging spallation failure, where the coating on brittle substrate (including WC-Co substrate as used in this test) detached in order to release compressive stress and minimize elastic energy stored in the coating ahead the indenter as it moves [29]. It indicates poor adhesion of coating to the substrate. This type of failure appears similar to recovery spalling which takes place behind the indenter and is caused by difference in modulus of substrate and coating. If the substrate has lower modulus than coating, during unloading they cannot relax at the same rate, leaving residual shear stress at the interface. Both wedging spallation and recovery spallation create cracks along the scratch track edges as visible in WTiN scratch, however the recovery spalling mode is not likely to be the case here because WTiN coating has lower modulus than WC-Co substrate.

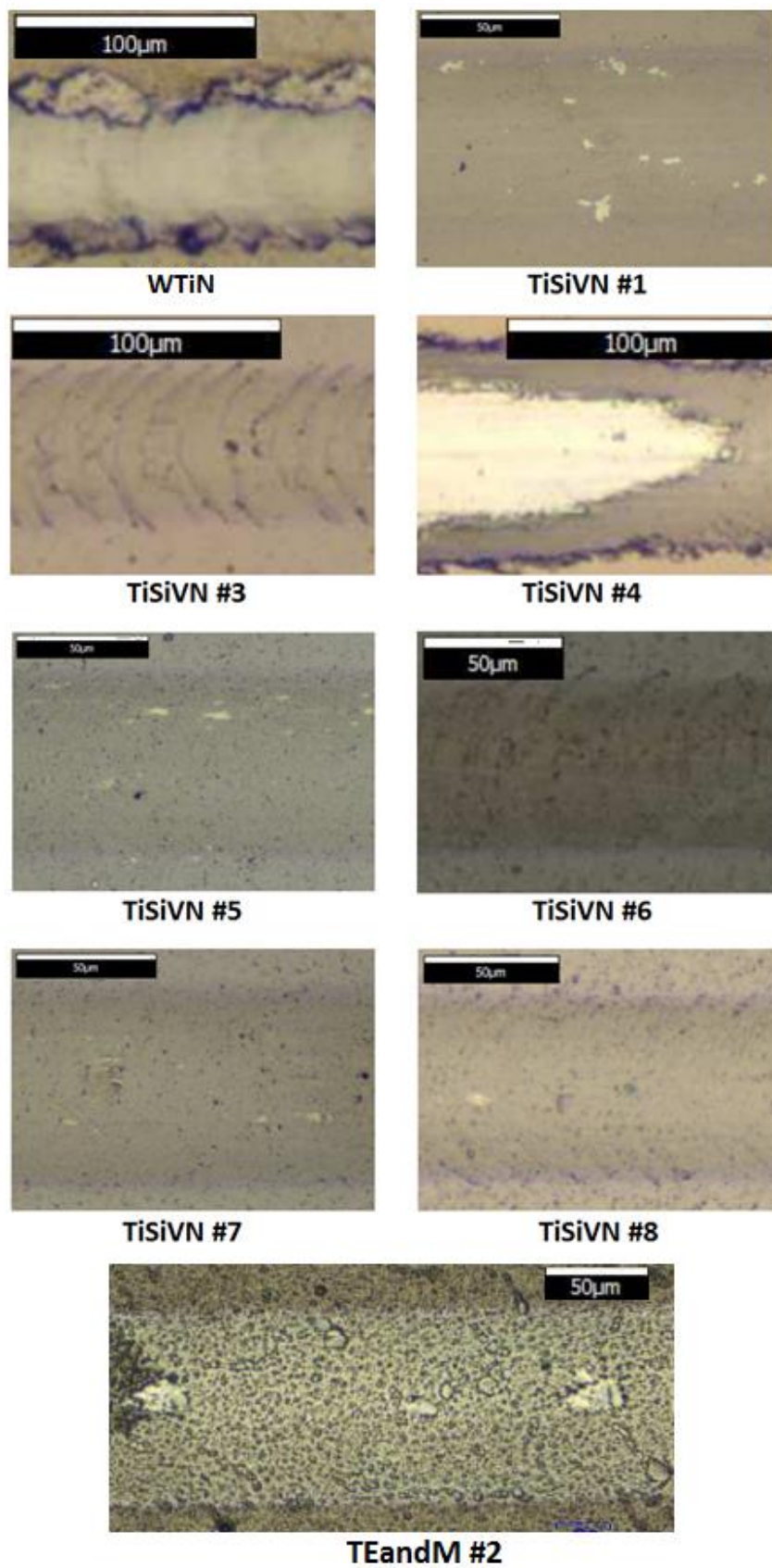


Figure 5.6. Failure modes on scratches of coatings (direction of indenter from right to left)

Most of TiSiVN coatings (excluding TiSiVN #2) and TEandM #2 coating had the same failure mode (yet to different extent), which was ductile buckling failures which occurred ahead of scratching indenter. This was a type of ductile failure due to the lack of adhesion where the coating buckled in front of the indenter as it moved forward [30]. Some parts of spalled coatings were then crushed and completely removed by the indenter as it passed, leaving some areas in the track where substrate was obviously exposed. The difference between this mode and compressive spallation (as demonstrated by WTiN) is that this failure occurs in ductile manner instead of brittle. Both occur due to compressive force ahead of the indenter, yet in ductile buckling the spallation is relatively small, confined within the scratch track and not significantly propagating to the edges.

In the case of weak adhesion but strong cohesion, arcs in the direction of indenter movement with minor amount of coating spallation were observable, such as in TiSiVN #3, #4, #6 and #8, until certain load was reached to completely tear off the coating from the substrate as happened in TiSiVN #4. On samples TiSiVN #1, #5 and #7, some spalls existed but the arc marks were not observable. It could be caused by stronger adhesion of coatings-substrate than cohesion within the coatings. Therefore, when the compressive stresses increased ahead of the indenter, instead of being dragged altogether, some parts that weakly adhered to the substrate were detached and removed as the indenter ran over it, leaving some spots where substrate was exposed, while the other parts still firmly attached to the substrate.

This scratch testing has provided insights on the adhesion (and cohesion) behaviors of coating. With some of coatings having stronger cohesion than adhesion and vice versa, TiSiVN #2 was proven to be the best among its kind in terms of this characteristic.

During machining operation, the system works in elevated temperature that can lower mechanical properties including the modulus of WC/Co, which effect also depends on its cobalt content [31]. Therefore, there is possibility for the failure to happen in different modes or severity compared to these tests.

5.3. Tribological performance of coatings

The results of ball on disk tests are discussed per each group of coatings for easier comparison and analysis of tribological characteristics. Those groups are as mentioned in the previous chapter: WTiN, TiSiVN with different deposition conditions and coatings produced by TEandM.

5.3.1. WTiN Coating

Friction coefficient (CoF) of WC ball coated with WTiN against Ti6Al4V in dry condition was higher than that of uncoated WC ball, as shown in Figure 5.7. The value of CoF was considered steady after 10 m and the average for uncoated and WTiN coated balls were 0.44 and 0.52, respectively. Dry friction coefficient value of WTiN here is similar to that obtained by Silva *et al.* [28] on dry ball on disk test of WTiN against high strength low-alloy steel and cold rolled steel, which was between 0.45 to 0.6. Approximately the same value of friction coefficient of uncoated WC, 0.45, was reported by Yetim *et al.* [34] on dry sliding of WC pin against Ti6Al4V disk, confirming the result of this test. The figures showing only the early stage (first short distance) of CoF vs distance are available in Appendix C to enable a closer view of the running-in period.

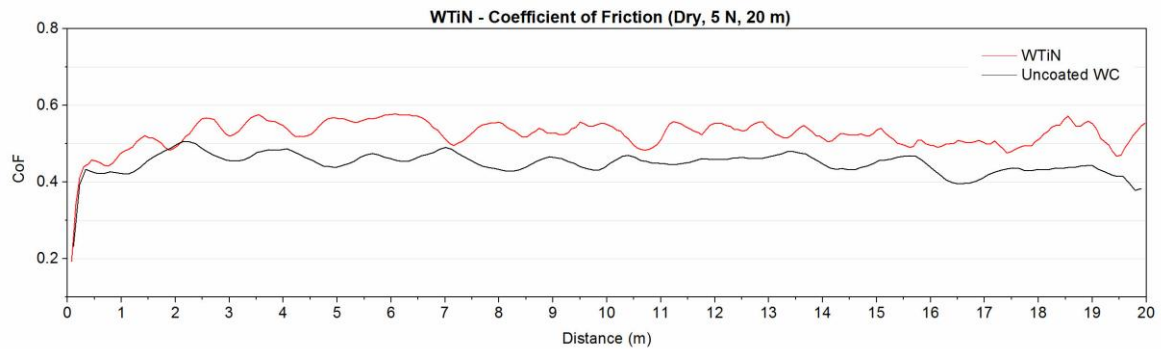


Figure 5.7. WTiN friction coefficient evolution on dry ball-on-disk test (5N load, 20 m linear distance)

Different behaviour was shown in lubricated test as plotted in Figure 5.8, where WTiN coated ball demonstrated lower friction coefficient than uncoated ball. In its steady state (50 m of 100 m test distance), WTiN coated ball recorded mean friction coefficient of 0.16, which was 20 % lower than the uncoated one (0.2). In addition, WTiN coated ball experienced shorter transient during the test as it dropped the friction coefficient to its steady values faster than the uncoated ball.

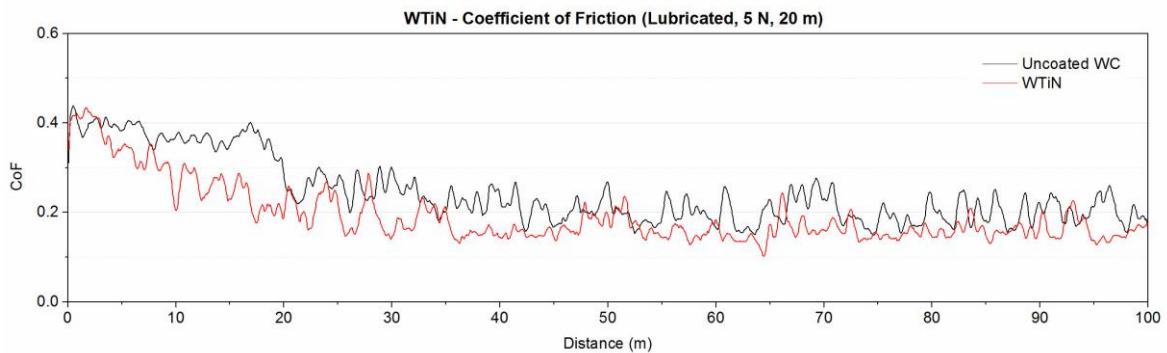


Figure 5.8. WTiN friction coefficient evolution on lubricated ball-on-disk test (5N load, 100 m linear distance)

Polynomial fitting of CoF vs distance chart in Figure 5.8 is presented in Figure 5.9, where the difference in friction coefficient and its evolution over the distance can be more clearly identified.

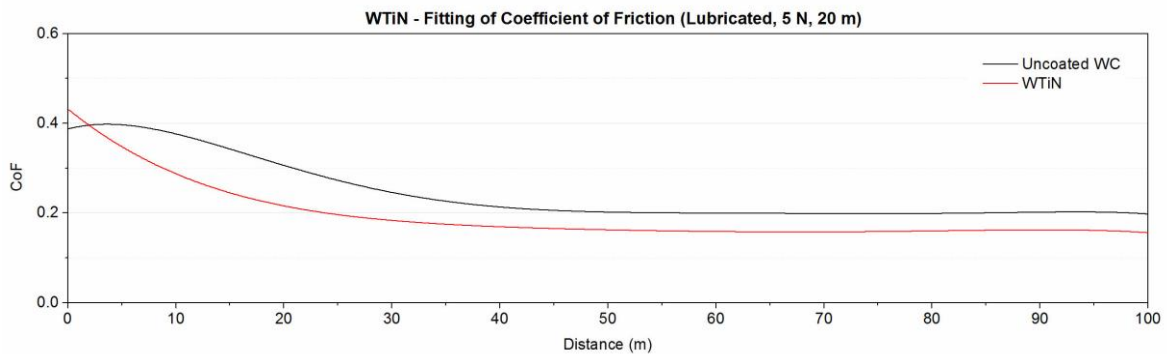


Figure 5.9. Polynomial fitting of WTiN friction coefficient evolution on lubricated ball-on-disk test (5N load, 100 m linear distance)

Investigation on balls wear scar revealed that both uncoated and coated ball had some adhered materials on it. From 3D profile measurement on the scar area, taking the fresh (untested) ball surface as reference surface, the volume above the reference was more prominent than the volume below. The 3D profiles of balls wear scars are presented in Figure 5.10 and 5.11. They clearly show the evidence of adhesion.

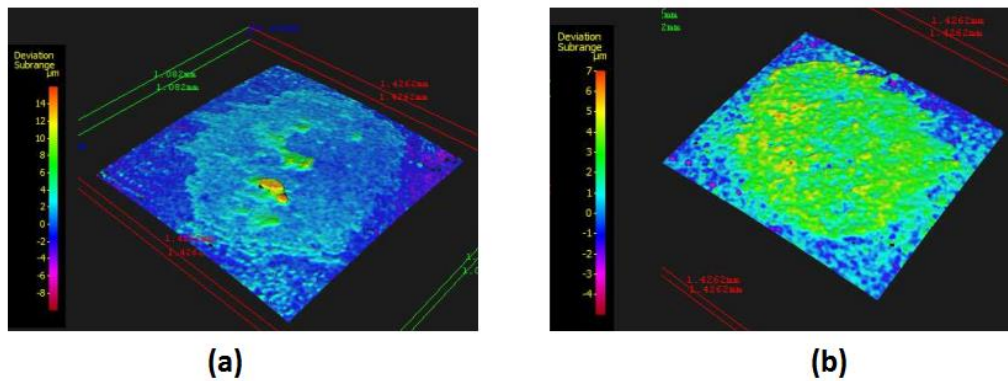


Figure 5.10. 3D profilometry of uncoated ball wear scar: (a) dry test; (b) lubricated test

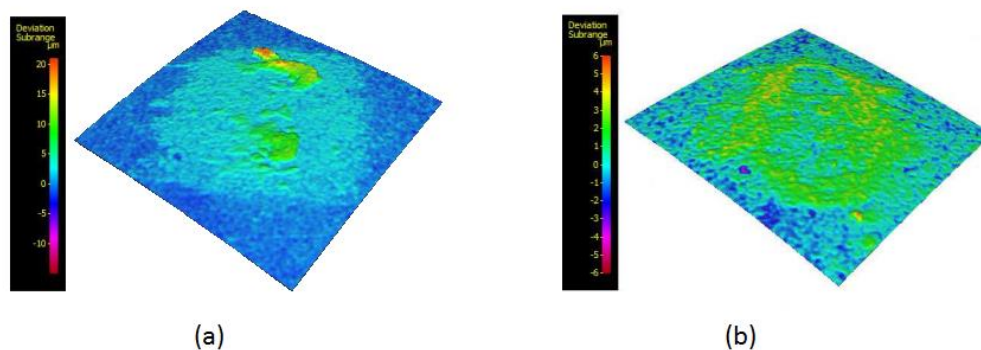


Figure 5.11. 3D profilometry of WTiN coated ball wear scar: (a) dry test; (b) lubricated test

The proportion of volume above and below reference (Figure 5.12) infers that there is adhesion of material from the disk instead of only deformation of ball material in wear scar area, because the measured volume above reference is much larger than that below. In the case of deformation that displaces some parts of deformed material, leaving valleys (volume below reference surface) behind and creating peaks (volume above reference) ahead, the difference in proportion of volume above and below will not be large because there is no incoming or outgoing volume, only displacement.

It was not known whether any wear existed underneath the volume of adhered material, i.e. the ball wore out first then the craters were filled with materials transferred from the counterface (Ti6Al4V disk) which continued to build up as the test went on. Because of the presence of this substantial adhesion also, calculation on wear rate of the ball scar could not be made. However, in this work, the volume above the reference surface as measured by 3D profilometer was considered as adhesion or material transfer and the volume below reference as wear.

In dry condition, adhesion was very significant on WTiN coating while in lubricated test its amount fell considerably. On the other hand, wear did not change significantly between dry and lubricated condition. The reverse phenomena appeared on

the uncoated ball: while adhesion relatively remained at the same amount, the wear decreased remarkably.

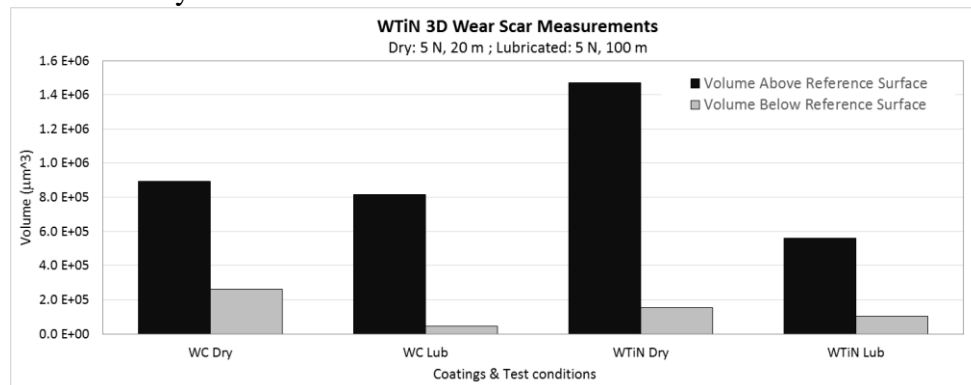


Figure 5.12. 3D profile volume calculation of balls wear scar

These test results are in line with previous investigation by Budinski [10] who concluded that in any sliding system, titanium had poor friction unless lubrication was present in the contact, either by liquid or solid/self-lubricating layer.

Wear track volume of the disk as presented in Figure 5.13 was calculated and expressed in specific wear rate (k). This term best serves as parameter that allow comparison between results of different load and/or distance as in these experiments where during dry test the linear distance was 20 m while it was 100 m during lubricated test. Despite having high adhesion on the ball, WTiN coating appeared to induce lower wear (material removal) on its Ti6Al4V counterface as compared to the uncoated one, which difference was more obvious in dry condition.

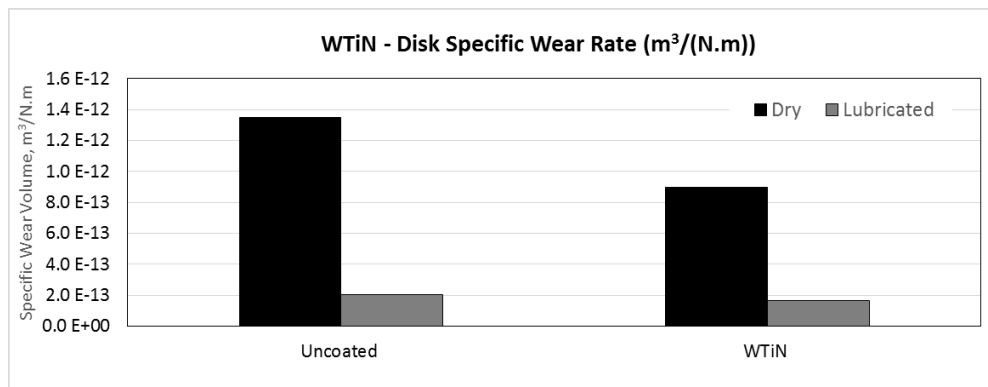


Figure 5.13. Wear track specific wear rate on Ti6Al4V disk, against WTiN coating

5.3.2. TiSiVN Coatings

The same manner of friction coefficient as happened in WTiN was also demonstrated by TiSiVN coatings, where at dry condition they performed poorly while once lubrication was introduced they were superior compared to the uncoated sample. The as-recorded chart of CoF vs distance and the polynomial fitting of it for dry and lubricated test are presented in Figure 5.14 and Figure 5.15, respectively. Polynomial fitting chart helps eliminating the waviness for easier analysis on the observation of mean and steady values while the as-recorded chart provides better resolution to see real features such as abrupt changes.

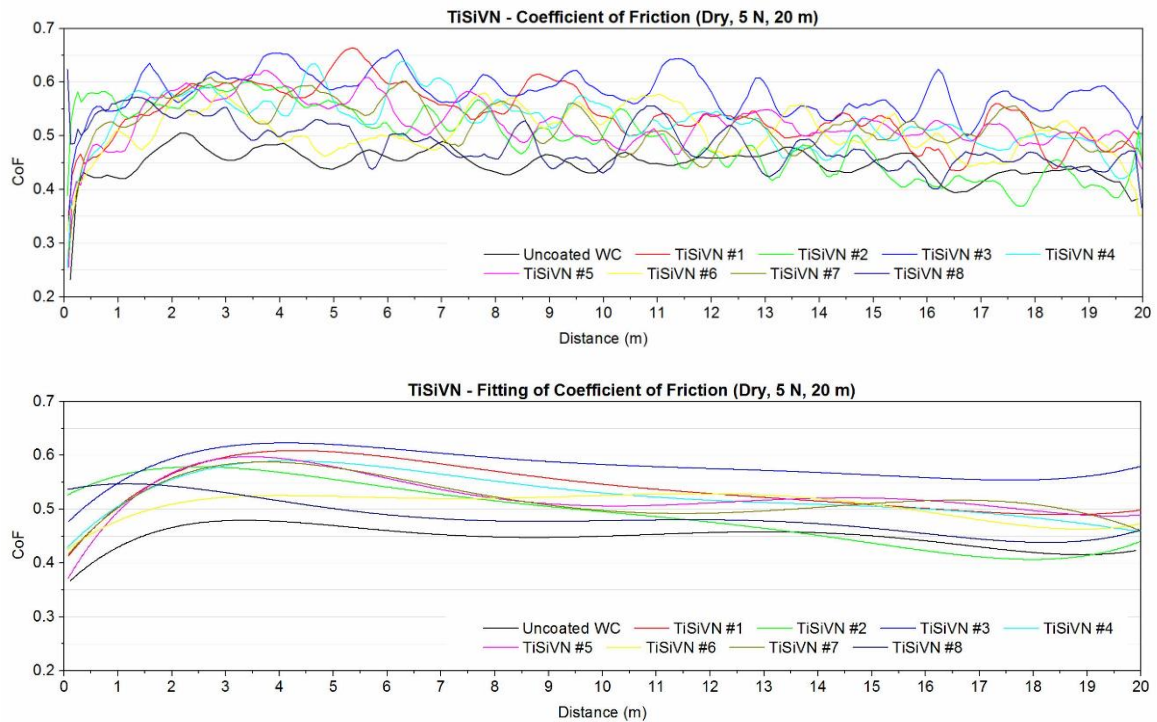


Figure 5.14. TiSiVN friction coefficient evolution on dry ball-on-disk test (5N load, 20 m linear distance)

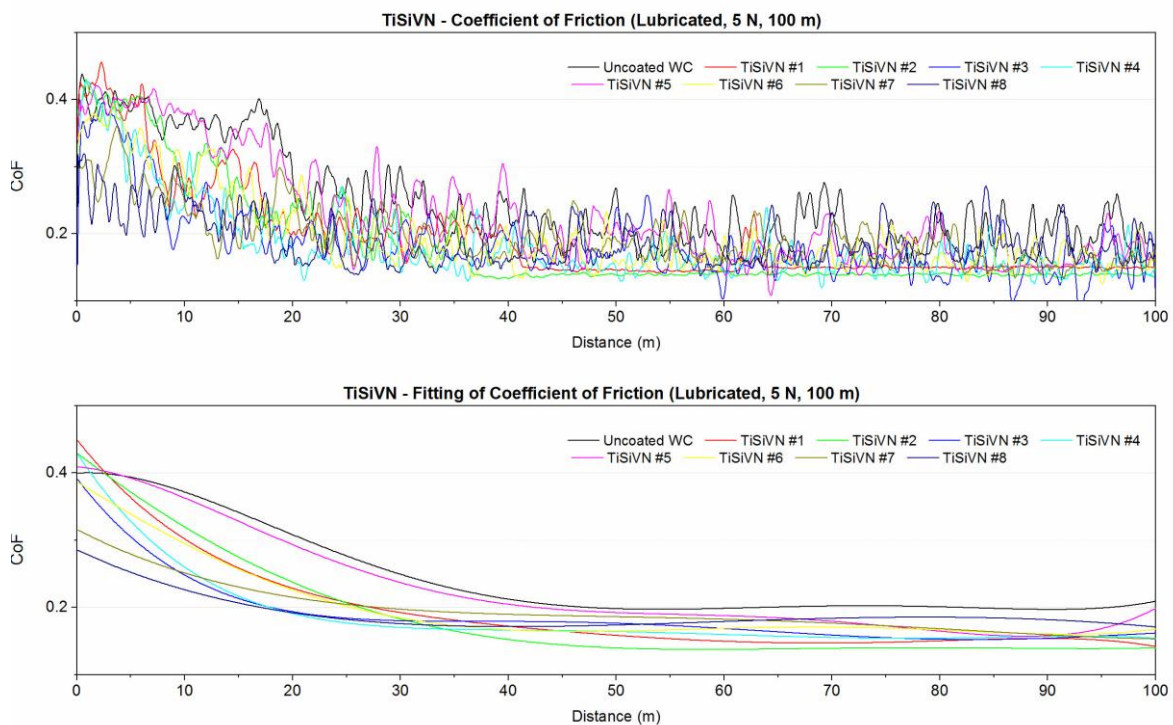


Figure 5.15. TiSiVN friction coefficient evolution on lubricated ball-on-disk test (5N load, 100 m linear distance)

Although it was not the same from coating to coating, steady value of CoF was taken from 10 m in dry conditions and 50 m in lubricated condition, where all of them were already considered to achieve their steady state. Noticeable behavior demonstrated by

TiSiVN #1 and #2 during lubricated test, they started at relatively high friction yet after gradual decrease they reached a point (42 m on #1 and 37 m on #2) where onwards they had not only very low friction coefficient but also very smooth fluctuation of it.

The comparison of steady state values of friction coefficient which can be seen in Figure 5.16 concludes that TiSiVN #2 is the best within this group. It has friction coefficient as low as uncoated ball in dry condition and much lower in lubricated. TiSiVN #1 is also good in lubricated condition, but it has high friction when dry.

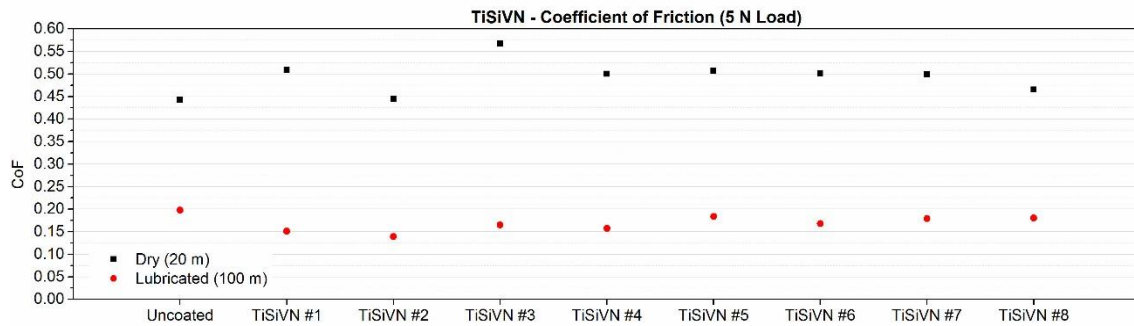


Figure 5.16 Steady state friction coefficient of TiSiVN samples on ball-on-disk test (5 N load)

With the same measurement techniques as in WTiN, the same behaviour also appeared in TiSiVN coatings, where material transfer dominated the ball wear scar, as inferred from the graph in Figure 5.17. A recent work on titanium transfer in dry sliding contact [32] came into conclusion that more transfer of material tends to create higher friction. While it was true on some samples, the statement contradicted some results in this experiment where lower material transfer appeared in coating with higher friction such as in TiSiVN #3, #4 and #6. This was possibly because besides adhesive mechanism, friction depends also on surface topography which contributes to ploughing mechanism. The topography of built-up transferred material might be significantly different in such way that it created more friction on some samples since it induced more ploughing mechanism.

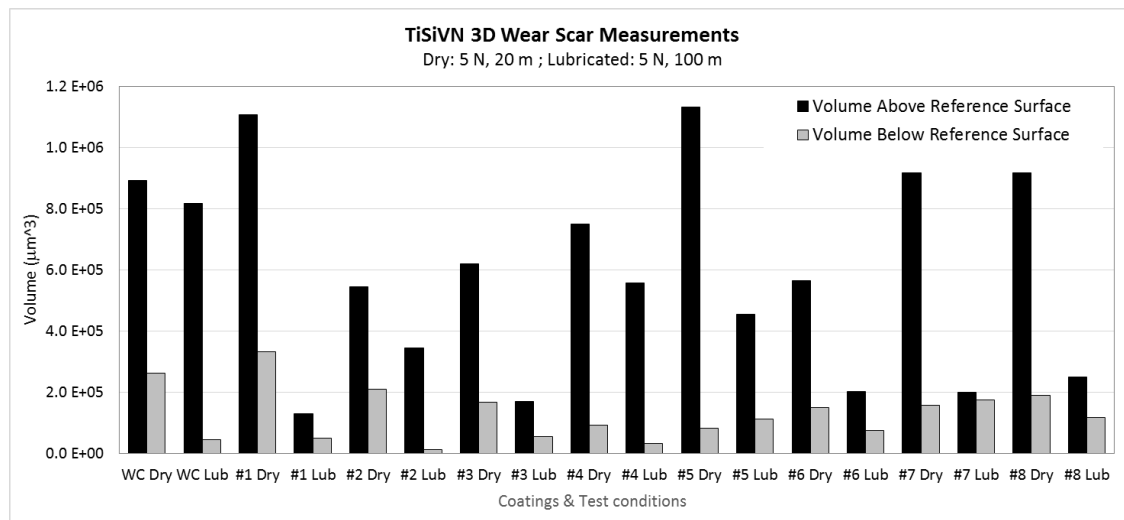


Figure 5.17. 3D profile volume calculation of TiSiVN coated balls wear scar

Looking at the wear rate of disk in Figure 5.18, sample #1 and #2 removed less material in lubricated test. This confirms the low friction and low wear characteristics of

those coatings. Low friction coefficient is very important to reduce forces and temperature on tool-workpiece interface that will affect the integrity of coating and tool.

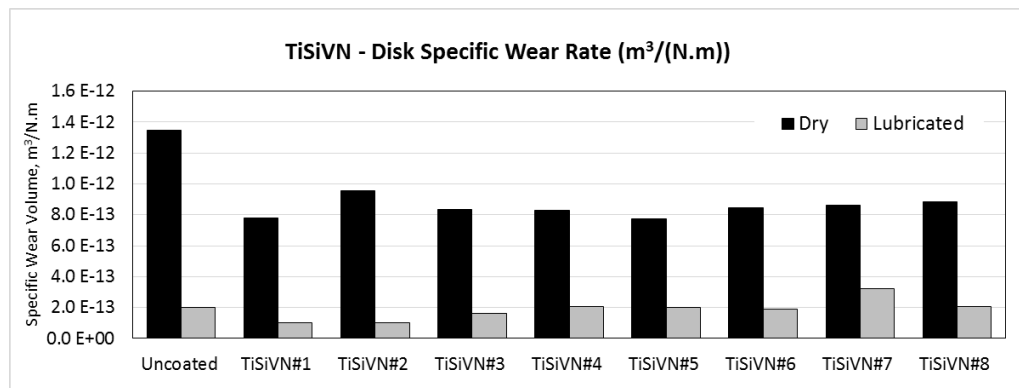


Figure 5.18. Wear track specific wear rate on Ti6Al4V disk, against TiSiVN coatings

5.3.3. Coatings from TEandM

In terms of friction coefficient, several kinds of behaviours demonstrated by the coatings from TEandM (Figures 5.19, 5.20 and 5.21). Steady state friction coefficient of sample TEandM #1 and #5 were similar to uncoated sample, in dry and lubricated condition. Sample TEandM #3 and #6 maintained friction coefficient lower than uncoated one in either conditions. The other samples, TEandM #2 and #4, showed almost the same values of friction coefficient, which were high in dry condition yet low when lubricated, compared to the uncoated sample.

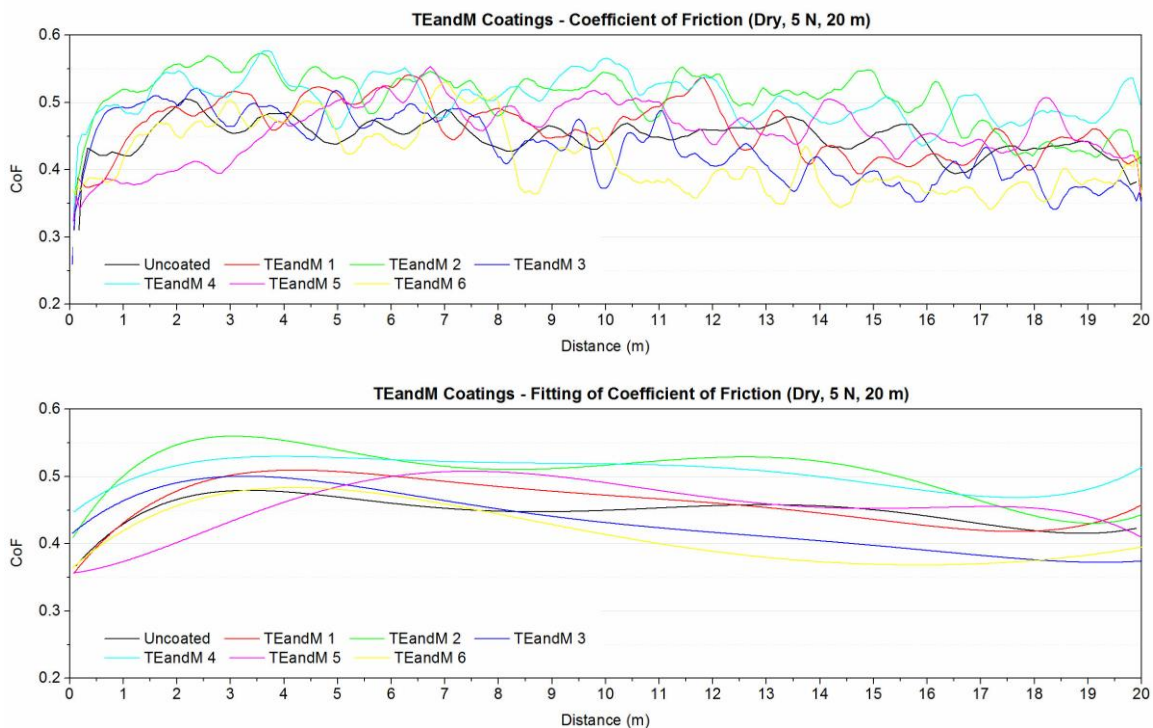


Figure 5.19. Friction coefficient evolution of TEandM produced coatings on dry ball-on-disk test (5N load, 20 m linear distance)

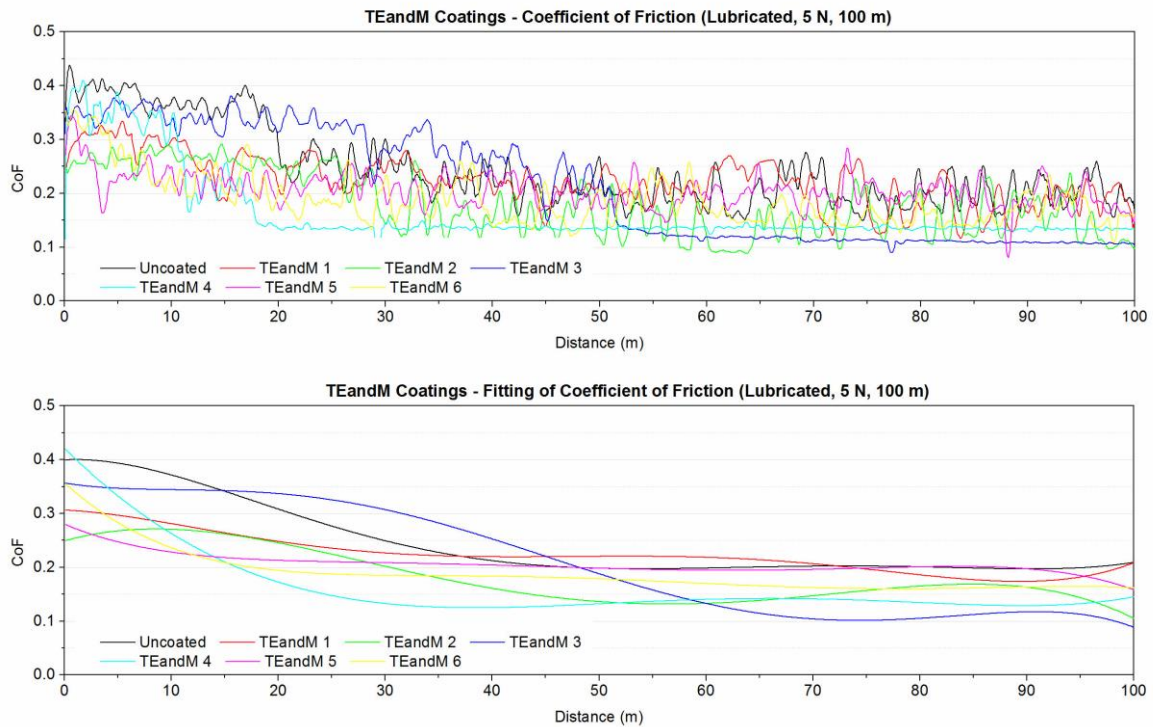


Figure 5.20. Friction coefficient evolution of TEandM produced coatings on lubricated ball-on-disk test (5N load, 20 m linear distance)

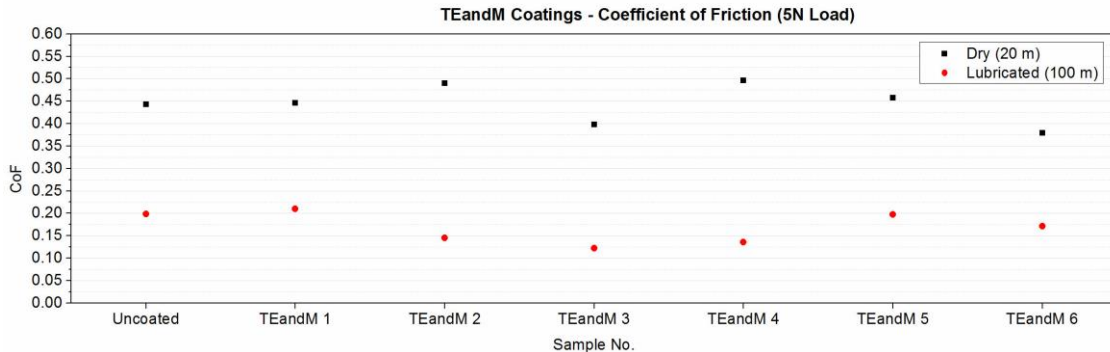


Figure 5.21. Steady state friction coefficient of TEandM coatings samples on ball-on-disk test (5N load)

Reviewing the chemical composition, sample TEandM #2 and #4 contain the same elements: N, Al, Si, Ti and Cr with approximately the same atomic percentages as well. This is probably the reason behind the similarity of friction behaviour between those coatings.

Although demonstrating the same friction coefficient, 3D profilometry on the ball showed that sample TEandM #1 and #5 had opposite wear characteristics. In TEandM #1 material transfer from the disk dominated the scar while in #5 material removal from ball surface was more dominant as seen in Figure 5.22. Sample TEandM #3 experienced very high wear during dry condition even though it had low friction coefficient, which was also occurred on sample #6.

Machining process of titanium is more likely to be carried out in a lubricated condition, yet there might be some instances of dry contact during the operation. Therefore, coatings that significantly wear out during dry condition are not preferable. In

this regard, coatings TEandM #2 and #4 provide good balance of material transfer and wear in both dry and lubricated conditions, compared to other coatings from TEandM.

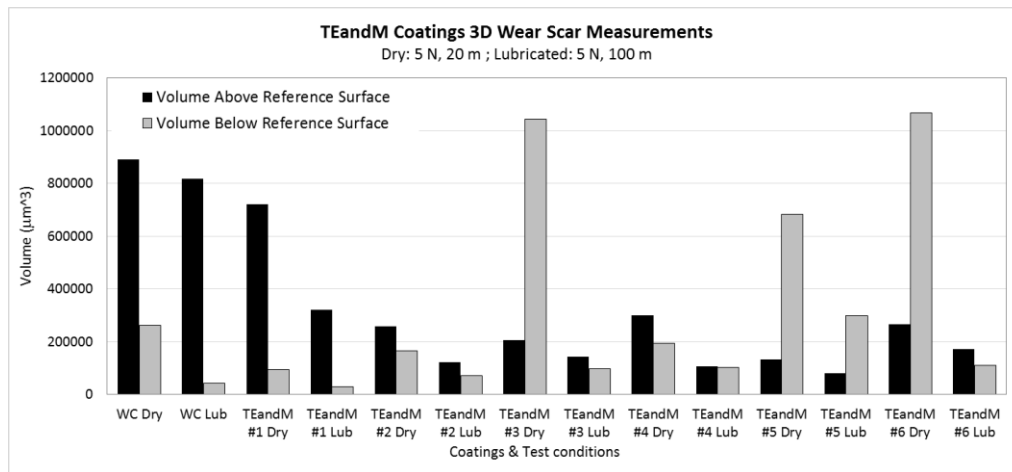


Figure 5.22. 3D profile volume calculation of TEandM coated balls' wear scar

With similar characteristics in friction and wear, which was most likely attributed to their similar elemental composition, TEandM #2 removes more material from its counterface compared to TEandM #4, as indicated by the graph in Figure 5.23.

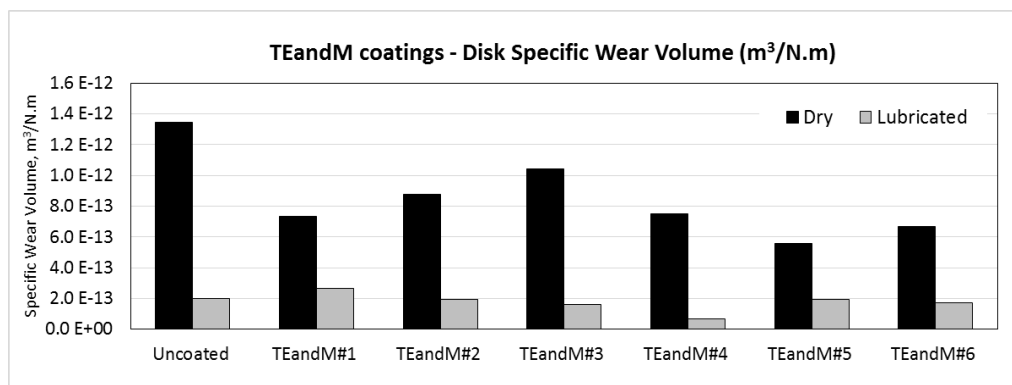


Figure 5.23. Wear track specific volume of Ti6Al4V disk, against TEandM coatings

5.4. Selection of coatings to be deposited on coating tools

While WTiN coating tested in this work is for sure to be deposited on cutting tool in the next stage of this project because it is the latest development of WTiN coating that can readily be made available in the Instituto Pedro Nunes, other coatings should be selected from their group, i.e. from TiSiVN types and from those supplied by TEandM.

The selection criteria of coatings include mechanical properties and tribological characteristics against Ti6Al4V, considering overall performance in terms of friction coefficient, cohesion and adhesion quality, wear of coating and material transfer onto its surface also the material removal of the counterface (disk). Selected coatings should provide optimum balance in characteristics suitable for cutting tool application.

In TiSiVN coatings group, TiSiVN #2 was found potential. Although it removed the least disk material on lubricated test, it had consistently low friction coefficient in both dry and lubricated conditions. Transfer (adhesion) of counterface material was also

relatively low without major difference between dry and lubricated condition as observed in other coatings. It allows more predictable behaviour of material transfer in different lubrication quantity, which is likely to occur during machining operation. Measured wear on the ball was low, especially when lubricated, which means that the expected coating life (thus tool life) can be longer. Calculated plasticity index of TiSiVN #2 is not the closest to the optimum value among TiSiVN, but it has the best cohesion and adhesion strength within the coating and to the substrate compared to other TiSiVN coatings as proven by the scratch test, which reflects its ability to maintain integrity when it slides under load.

From all the coatings produced by TEandM, sample TEandM #2 and #4 were proved, tribologically, to be the potential candidates for tool coatings. Their friction coefficients were rather high when dry, but dropped considerably in lubricated condition which is supposed to be the desired condition in most of machining processes. Also, they showed good balance of material transfer and wear as compared to other coatings from TEandM. Material transfer in machining process, which appears as chip adhesion to cutting edge, increases workpiece surface roughness while the wear shortens tool life, therefore excessive amount of either is not preferable. Only one coating from TEandM was tested for mechanical and adhesion properties, TEandM #2, which was the best tribologically compared to other coatings produced by TEandM. It has better adhesion than WTiN although not as good as TiSiVN #2.

Friction and wear characteristics for the selected coatings are summarized in Figures 5.24, 5.25 and 5.26. Selected coatings have friction coefficient values and track specific wear rate that are close to each other.

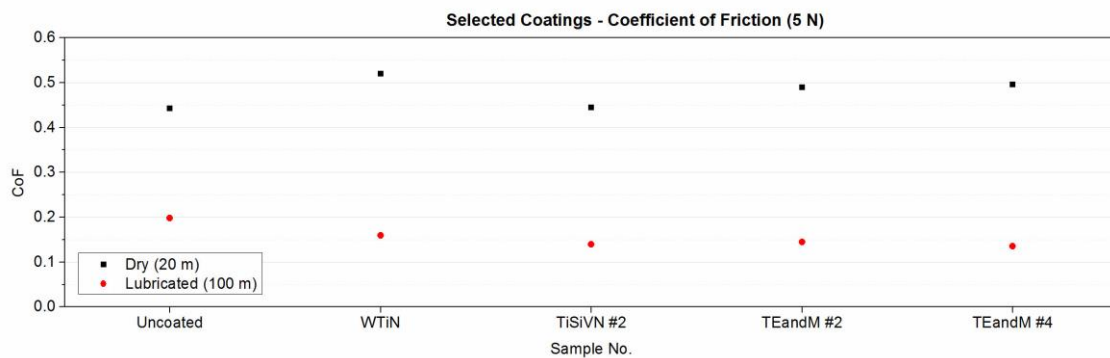


Figure 5.24. Friction coefficients of selected coatings

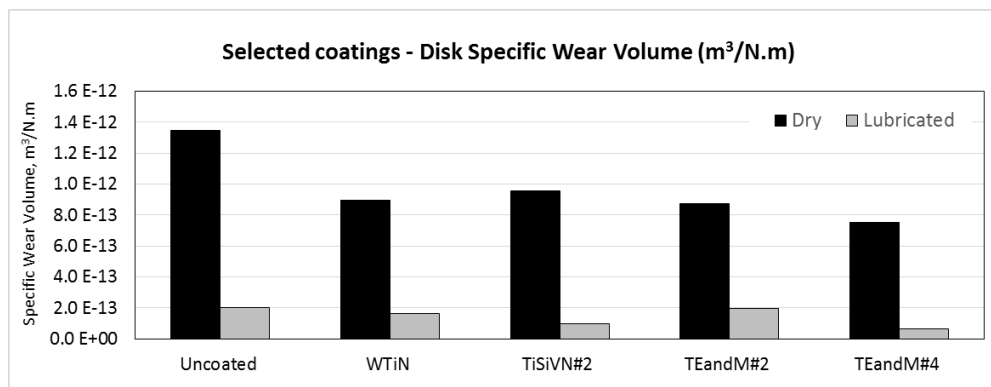


Figure 5.25. Specific wear rate of Ti6Al4V disks against selected coatings

Significant difference between coatings is found in the ball wear scar, where coatings from TEandM have less material transfer. That is possibly related to strong

adhesive behavior of Ti, especially on dry sliding [10,32,33]. WTiN and TiSiVN#2 have high content of Ti: 28 at% and 32 at%, respectively. On the other hand, samples TEandM #2 and #4 from have much lower Ti content which are around 4 at%. On the tested samples, more Ti content in the coatings caused higher adhesion. However, in TiSiVN, the presence of V compensated adverse tribological characteristic of Ti by acting as solid lubricant. Therefore, although TiSiVN#2 still created material transfer higher than TEandM coatings (which obviously have lower Ti content), the amount was substantially lower than that of WTiN (which has only slightly less Ti). In addition, friction coefficient of TiSiVN#2 was also considerably low, which was clearly noticeable during dry condition, suggesting the effect of dry lubrication contributed by V.

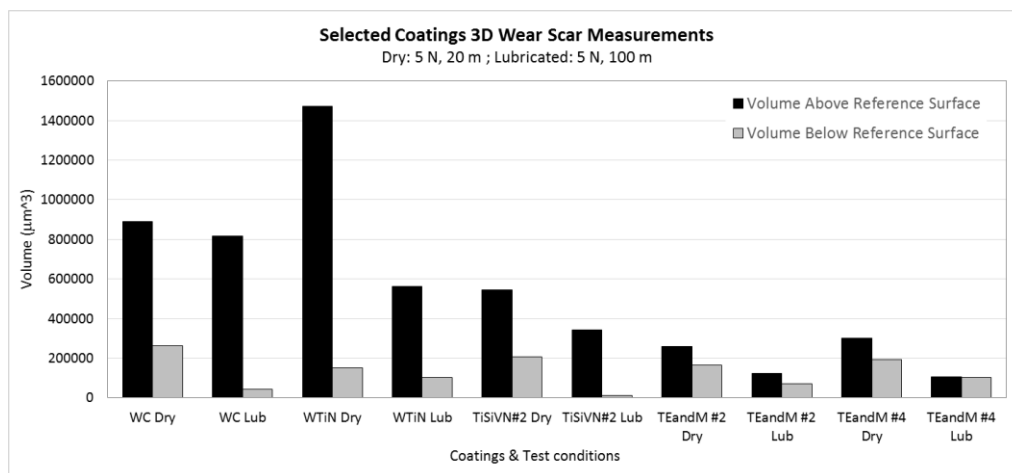


Figure 5.26. 3D measurements of ball wear scar of selected coatings

6. PREPARATORY PROCEDURE FOR FINAL TESTING OF COATED SAMPLE: TOOL GEOMETRY SELECTION

As the aim of Comptitool project is to develop coated cutting tools, selection of tool geometry is also important in order to gain an optimum outcome by combining the quality of coating and tool geometry.

6.1. Tested geometries

In this work, three prototypes of milling tools of different geometries, supplied by a company (Frezite), were tested on CNC machine. Tools are uncoated WC-Co, with diameter of 12 mm. Each of tools has 4 cutting edges, yet with different geometry. Figure 6.1 depicts top view of cutting tools observed under optical microscope, showing the cutting edges of each tool with its corresponding prototype designation.



Figure 6.1. Prototypes of milling tools being tested

6.2. Test methods and conditions

A Kistler 9123C dynamometer as illustrated in Figure 6.2, was mounted on the spindle of CNC machine. The tool was held on the tool holder at the bottom side of dynamometer. This dynamometer logged the forces and moment during machining tests.



Figure 6.2. Kistler 9123C dynamometer

Shoulder milling was performed by each tool prototype on Ti6Al4V block of 150 mm x 100 mm x 50 mm size. For every tool, two phases of test were conducted. Each phase was done with the same machining parameters. Tool was observed and measured with 3D profilometer after each phase.

Machining parameters were determined based on previous tests, choosing the value that resulted in longer tool life and good workpiece finish. Some parameters were also set above the common practice to set a higher test standard. Details of parameters used in the test is elaborated in Table 6.1.

Table 6.1. Machining parameters used in shoulder milling tests

Tool diameter	12 mm
Spindle speed (n)	4000 rpm
Cutting speed (v_c)	150 m/min
Depth of cut (a_p)	15 mm
Working engagement (a_e)	1.2 mm
Table feed (v_f)	1200 mm/min
Number of cutting edges	4
Feed per rev (f_n)	0.075 mm/rev
External lubrication	Cutting fluid
Pressure	10 bar
Linear length – Phase 1	5.25 m
Linear length – Phase 2	5.25 m
Total tool travel	10.5 m
Material removal rate (RMR)	21.6 cm ³ /min

6.3. Test results

6.3.1. Force and moment

The linear length of 5.25 m at each phase were completed after 35 passes (150 mm per pass). Axial force (force parallel with tool's axis) and moment about z-axis (tool's axis) were logged during machining process.

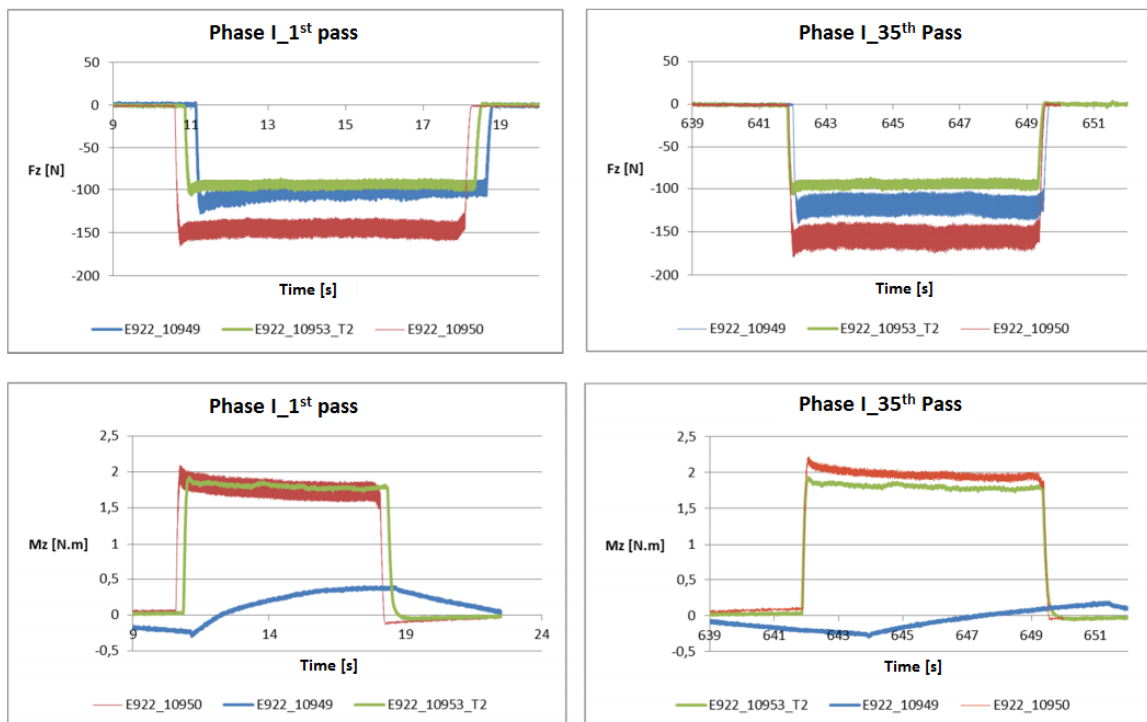


Figure 6.3. Force and moment during first phase of test

Graphs in Figure 6.3 show that prototype E922_10950 has highest magnitude of axial force than the others (negative value indicates downward direction). Some increases of force and moment can also be observed in the graphs after 35 passes. An erratic signal of moment appeared during the test of E922_10949, as shown in the chart, thus no specific information can be drawn.

In the second phase of the test (Figure 6.4), prototype E922_10953 could only make 27 passes before it broke, therefore covered only 9 m of total linear travel combined with the first phase, out of 10.5 m of planned length. Low axial force and high moment exhibited at the last pass of the failed prototype E922_10953. Other prototypes had similar force behaviour to what happened in phase 1 where E922_10950 being the highest, followed by E922_10949. The moment for E922_10949 was able to be logged in this second phase, where its magnitude increased over the phase at higher rate than E922_10950.

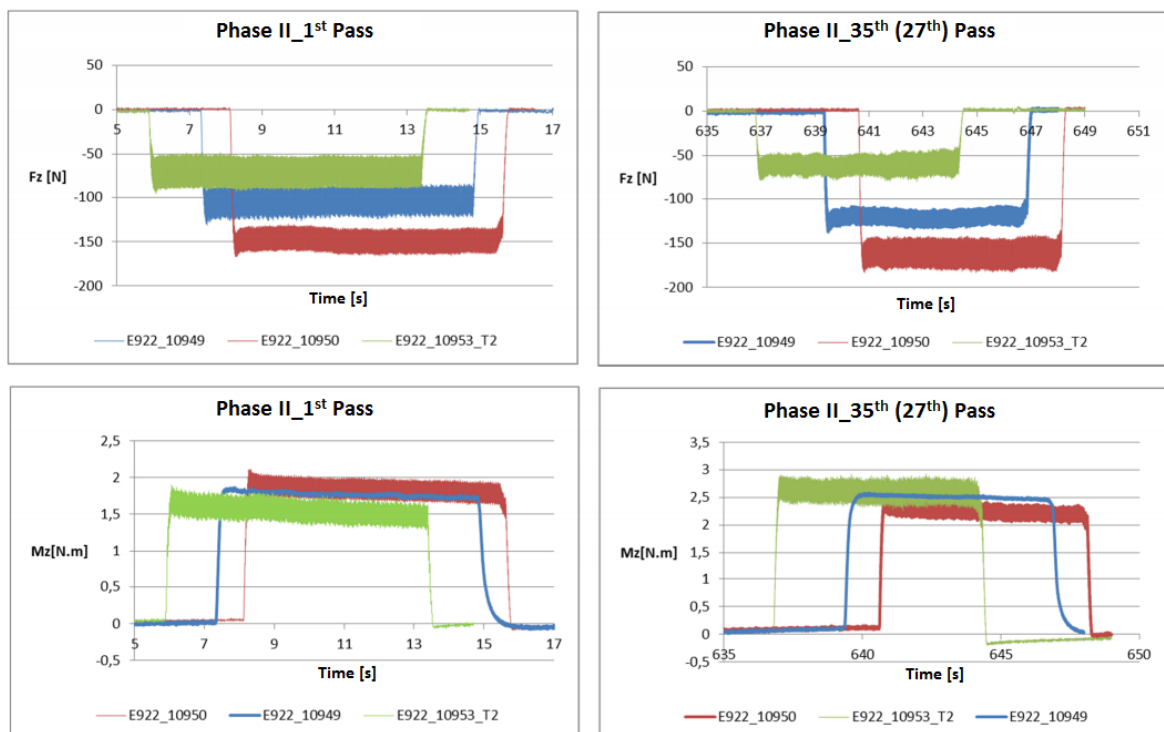


Figure 6.4. Force and moment during second phase of test

Overall, in the point of view of machining forces, prototype E922_10950 had consistent behavior over the length of test in terms of changes in force and moment, although it induced more forces. E922_10949 had more increase in force and more prominently, in moment, suggesting the occurrence of wear. The lowest force and moment were exhibited by prototype E922_10953, however it had poor durability as it broke early during the test.

6.3.2. Wear of cutting edges

Before the first phase and after each phase, cutting edges were measured for wear under optical microscope with 3D profilometer. The tools have 4 cutting edges with the opposing pairs having the same geometry that can be different with another pair on their right angle. In the figures and analysis that follows, those pairs are designated as cutting edges number 1 and 2.

Flank wear, V_b , of cutting edges were measured after each machining test phase, except after the second phase of E922_10953 which broke during the test. The end of tool life criterion is at the flank wear of 200 μm .

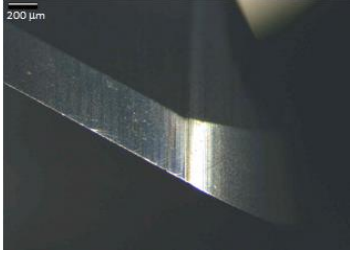
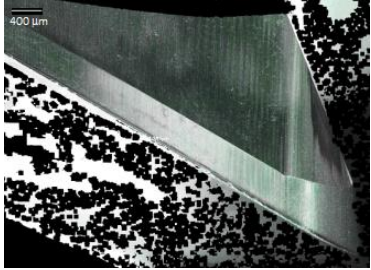
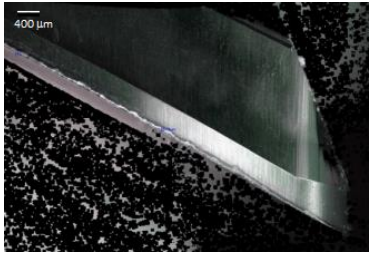
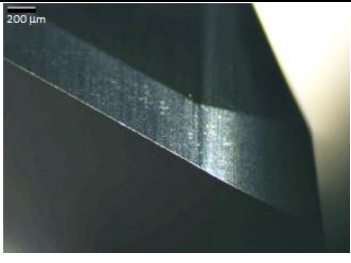
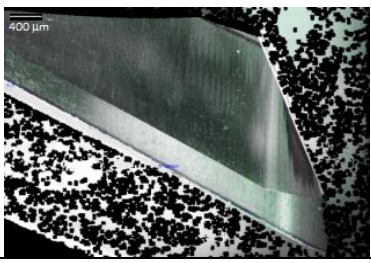
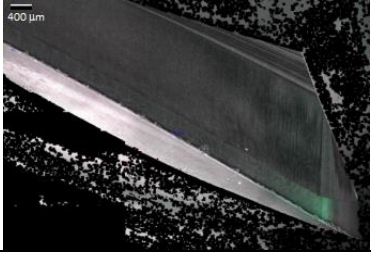
	New	After Phase I	After Phase II
1			
		$V_b = 44.3 \mu\text{m}$	$V_b = 116 \mu\text{m}$
2			
		$V_b = 54.2 \mu\text{m}$	$V_b = 225.5 \mu\text{m}$

Figure 6.5. Flank wear on prototype E922_10949 (1st row: cutting edge#1; 2nd row: cutting edge #2)

One of cutting edges of E922_10949 had flank wear of 225 μm after the end of second phase (10.5 m of covered linear distance) with several large chippings. The other cutting edge had only 116 μm of flank wear, with smaller chippings and deformations distributed along the edge.

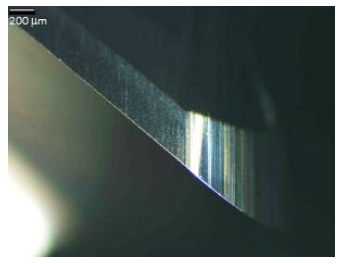
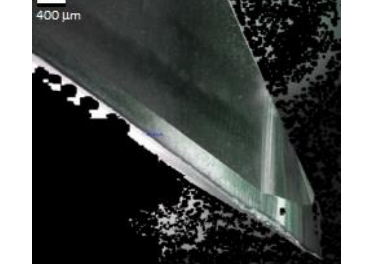
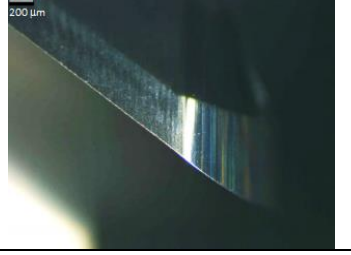
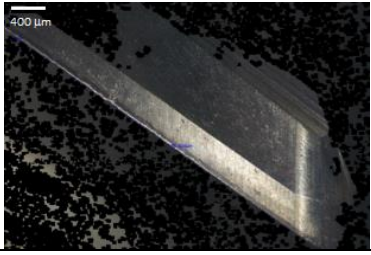
	New	After Phase I	After Phase II
1			
		$V_b = 0 \mu\text{m}$	$V_b = 105 \mu\text{m}$
2			
		$V_b = 56 \mu\text{m}$	$V_b = 132 \mu\text{m}$

Figure 6.6. Flank wear on prototype E922_10950 (1st row: cutting edge#1; 2nd row: cutting edge #2)

The E922_10950 prototype did not reach its life limit after 10.5 m, with flank wear still lower than 200 μm . Based on flank wear measurement, this prototype was better than E922_10949 since it had lower V_b value and there was no cutting edge went beyond tool life limit criterion. However, wear on the corner of E922_10950 cutting edge after the second phase was more severe than that of E922_10949 (compare Figures 6.5 and 6.6).

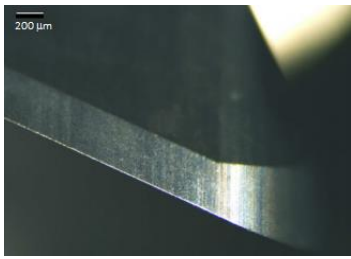
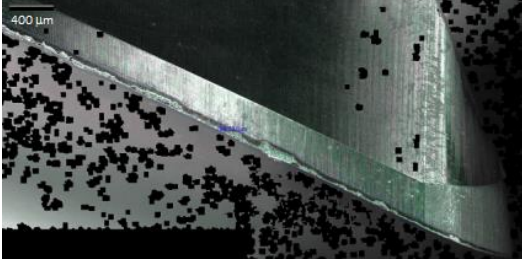
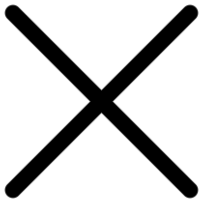
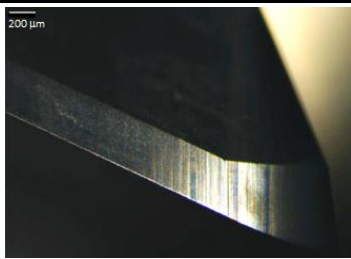
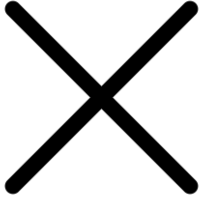
	New	After Phase I	After Phase II
1			
		$V_b = 99.5 \mu\text{m}$	Tool broke
2			
		$V_b = 131 \mu\text{m}$	Tool broke

Figure 6.7. Flank wear on prototype E922_10953 (1st row: cutting edge #1; 2nd row: cutting edge #2)

Significant wear on the failed tool, E922_10953 had been obvious after first phase (5.25 m linear travel) as shown in Figure 6.7, where it experienced wear twice the width as the other prototypes.

6.3.3. Surface roughness of finished workpiece

Surface roughness of workpiece as measured by 2D profilometer are presented in Table 6.2 as the average arithmetic roughness, R_a , and mean roughness depth, R_z (DIN). From the table, it is clear that prototype E922_10950 produced lowest and consistent surface roughness machined workpiece along the test length. Prototype E922_10953, which only make 9 m linear distance before it broke, produced rougher surface. Although its R_a was rather low after the second phase, but its R_z remained highest which reflected the presence of bigger asperities.

Table 6.2. Surface roughness of finished workpiece resulted by different tool

Tool Prototype	Phase I		Phase II	
	R_a (μm)	R_z (μm)	R_a (μm)	R_z (μm)
E922_10949	0.5	4.0	0.9	6.2
E922_10950	0.4	3.2	0.5	3.7
E922_10953	0.8	5.8	0.6	7.1

6.4. Summary of tool geometry selection

Considering the test results, prototype E922_10949 and E922_10950 were chosen to be coated with the coatings selected in the last section of previous chapter (WTiN, TiSiVN #2 and TEandM #2 or TEandM #4). Those two geometries demonstrated longer tool life as reflected by their flank wear measurements, although their machining forces were higher than the failed prototype. Surface roughness of workpiece machined with those two prototypes were also low, especially E922_10950 which maintained consistently low roughness throughout the tests.

7. CONCLUSIONS

A series of tests and measurements conducted in this study have revealed the tribological behaviour of the investigated coatings against Ti6Al4V. Based on the results, several coatings have been considered as outperformers thus selected for further research where they are to be deposited on cutting tools and tested in machining operations.

Summing up the results of coatings evaluation, the following conclusions can be drawn:

1. Among the tested coatings, TiSiVN with 7% Si deposited at 28.31 kW peak power (HiPIMS) with 5 pellets of vanadium (TiSiVN #2) had superior cohesion-adhesion properties within the coating and to the substrate although its plasticity index was not the best. Future research to tailor plasticity index parameter, which linked to hardness and modulus, would be valuable for the development of better coatings.
2. Common behaviour was found on most of the investigated coatings in sliding against Ti6Al4V that they had high friction coefficient in dry condition yet low in lubricated condition, as compared to uncoated WC-Co. This fact is in line with findings of other authors regarding poor friction characteristics of titanium in unlubricated tribosystem. Two tested coatings indeed showed low friction in dry test, but they had high wear rate hence less potential to be used in this application.
3. Ti6Al4V adhesion to its counterface was obvious. It dominated the balls wear scars as observed by 3D measurement. Wear also existed on the balls, but a valid measurement could not be made due to the abundance of adhesion.
4. All in all, out of 8 TiSiVN coatings, TiSiVN #2 was found to be the best. From TEandM, coatings TEandM #2 (HARD SILK) and TEandM #4 (HARD SILK II) were deemed to be the most potential ones, with the preference to TEandM #2. Those selected coatings, along with WTiN, are to be deposited on tools and tested on machining operations at the next stage of this project.

As a preparation for subsequent work, selection of cutting tool prototypes (milling tool) of different geometries has been carried out to obtain the optimum shapes of tools which together with selected coatings are expected to create cutting tools with improved performance. Two types of milling cutter have been chosen to be deposited with the selected coatings, based on their longer tool life and better workpiece surface finish in milling tests.

REFERENCES

- [1] A.P. Mouritz, Introduction to aerospace materials, in: *Introd. Aerosp. Mater.*, Woodhead Publishing Limited, Philadelphia, 2012. doi:10.5124/jkma.2012.55.7.649.
- [2] V.S. Kosaraju, B. Popuri, Taguchi Analysis on Cutting Forces and Temperature in Turning Titanium Ti-6Al-4V, *Int. J. Mech. Ind. Eng.* 1 (2012) 55–59. https://www.idc-online.com/technical_references/pdfs/mechanical_engineering/Taguchi_Analysis.pdf.
- [3] E.O. Ezugwu, J. Bonney, Y. Yamane, An overview of the machinability of aeroengine alloys, *J. Mater. Process. Technol.* 134 (2003) 233–253. doi:10.1016/S0924-0136(02)01042-7.
- [4] Ahmad Yasir M.S, Che Hassan C.H, Jaharah A.G, Nagi H.E, Yanuar B, Gusri A.I, Machinability of Ti-6Al-4V Under Dry and Near Dry Condition Using Carbide Tools, *Open Ind. Manuf. Eng. J.* 2 (2009) 1–9. doi:10.2174/1874152500902010001.
- [5] A. Jawaid, C.H. Che-Haron, A. Abdullah, Tool wear characteristics in turning of titanium alloy Ti-6246, *J. Mater. Process. Technol.* 92-93 (1999) 329–334. doi:10.1016/S0924-0136(99)00246-0.
- [6] C.H. Che-Haron, Tool life and surface integrity in turning titanium alloy, *J. Mater. Process. Technol.* 118 (2001) 231–237.
- [7] P.-J. Arrazola, A. Garay, L.-M. Iriarte, M. Armendia, S. Marya, F. Le Maitre, Machinability of titanium alloys (Ti6Al4V and Ti555.3), *J. Mater. Process. Technol.* 9 (2008) 2223–2230. doi:10.1016/j.jmatprotec.2008.06.020.
- [8] E.O. Ezugwu, Z.M. Wang, Titanium alloys and their machinability, *J. Mater. Process. Technol.* 68 (1997) 262–274. doi:10.1016/S0924-0136(96)00030-1.
- [9] Q.L. Niu, X.H. Zheng, W.W. Ming, M. Chen, Friction and Wear Performance of Titanium Alloys against Tungsten Carbide under Dry Sliding and Water Lubrication, *Tribol. Trans.* (2012) 121005134816006. doi:10.1080/10402004.2012.729296.
- [10] K.G. Budinski, Tribological properties of titanium alloys, *Wear.* 151 (1991) 203–217. doi:10.1016/0043-1648(91)90249-T.
- [11] M. Rahman, Y.S. Wong, A.R. Zareena, Machinability of Titanium Alloys., *JSME Int. J.* 46 (2003) 107–115. doi:10.1299/jsmec.46.107.
- [12] A. Jawaid, S. Sharif, S. Koksai, Evaluation of wear mechanisms of coated carbide tools when face milling titanium alloy, *J. Mater. Process. Technol.* 99 (2000) 266–274. doi:10.1016/S0924-0136(99)00438-0.
- [13] S. Pervaiz, A. Rashid, I. Deiab, M. Nicolescu, Influence of Tool Materials on Machinability of Titanium- and Nickel-Based Alloys: A Review, *Mater. Manuf. Process.* 29 (2014) 219–252. doi:10.1080/10426914.2014.880460.
- [14] R. Komanduri, W.R. Reed, Evaluation of carbide grades and a new cutting geometry for

- machining titanium alloys, *Wear*. 92 (1983) 113–123. doi:10.1016/0043-1648(83)90011-X.
- [15] G. Sutter, G. List, Very high speed cutting of Ti-6Al-4V titanium alloy - Change in morphology and mechanism of chip formation, *Int. J. Mach. Tools Manuf.* 66 (2013) 37–43. doi:10.1016/j.ijmachtools.2012.11.004.
- [16] S. Vijay, V. Krishnaraj, Machining Parameters Optimization in End Milling of Ti-6Al-4V, *Procedia Eng.* 64 (2013) 1079–1088. doi:10.1016/j.proeng.2013.09.186.
- [17] R.B. Da Silva, Á.R. Machado, E.O. Ezugwu, J. Bonney, W.F. Sales, Tool life and wear mechanisms in high speed machining of Ti-6Al-4V alloy with PCD tools under various coolant pressures, *J. Mater. Process. Technol.* 213 (2013) 1459–1464. doi:10.1016/j.jmatprotec.2013.03.008.
- [18] E. Bagci, B. Ozcelik, Effects of different cooling conditions on twist drill temperature, *Int. J. Adv. Manuf. Technol.* 34 (2007) 867–877. doi:10.1007/s00170-006-0668-2.
- [19] A. Shokrani, V. Dhokia, S.T. Newman, Environmentally conscious machining of difficult-to-machine materials with regard to cutting fluids, *Int. J. Mach. Tools Manuf.* 57 (2012) 83–101. doi:10.1016/j.ijmachtools.2012.02.002.
- [20] L.N. López De Lacalle, J. Pérez, J.I. Llorente, J.A. Sánchez, Advanced cutting conditions for the milling of aeronautical alloys, *J. Mater. Process. Technol.* 100 (2000) 1–11. doi:10.1016/S0924-0136(99)00372-6.
- [21] S. Sharif, E.A. Rahim, Performance of coated- and uncoated-carbide tools when drilling titanium alloy-Ti-6Al4V, *J. Mater. Process. Technol.* 185 (2007) 72–76. doi:10.1016/j.jmatprotec.2006.03.142.
- [22] A. Leyland, A. Matthews, On the significance of the H/E ratio in wear control: A nanocomposite coating approach to optimised tribological behaviour, *Wear*. 246 (2000) 1–11. doi:10.1016/S0043-1648(00)00488-9.
- [23] B.D. Beake, G.S. Fox-Rabinovich, S.C. Veldhuis, S.R. Goodes, Coating optimisation for high speed machining with advanced nanomechanical test methods, *Surf. Coatings Technol.* 203 (2009) 1919–1925. doi:10.1016/j.surfcoat.2009.01.025.
- [24] F. Fernandes, J. Morgiel, T. Polcar, A. Cavaleiro, Oxidation and diffusion processes during annealing of TiSi(V)N films, *Surf. Coatings Technol.* 275 (2015) 120–126. doi:10.1016/j.surfcoat.2015.05.031.
- [25] J.H. Ouyang, T. Murakami, S. Sasaki, High-temperature tribological properties of a cathodic arc ion-plated (V,Ti)N coating, *Wear*. 263 (2007) 1347–1353. doi:10.1016/j.wear.2006.12.031.
- [26] W. Tillmann, S. Momeni, F. Hoffmann, A study of mechanical and tribological properties of self-lubricating TiAlVN coatings at elevated temperatures, *Tribol. Int.* 66 (2013) 324–329. doi:10.1016/j.triboint.2013.06.007.
- [27] F. Fernandes, T. Polcar, A. Cavaleiro, Tribological properties of self-lubricating TiSiVN

- coatings at room temperature, *Surf. Coatings Technol.* 267 (2015) 8–14. doi:10.1016/j.surfcoat.2014.10.016.
- [28] P.N. Silva, J.P. Dias, A. Cavaleiro, Performance of W-TI-(N) coated pins in lubricated pin-on-disk tests, *Surf. Coatings Technol.* 202 (2008) 2338–2343. doi:10.1016/j.surfcoat.2007.09.039.
- [29] S.J. Bull, Failure Mode Maps in the Thin Scratch Adhesion Test, *Tribol. Int.* 30 (1997) 491–498.
- [30] S.J. Bull, Failure modes in scratch adhesion testing, *Surf. Coatings Technol.* 50 (1991) 25–32. doi:10.1016/0257-8972(91)90188-3.
- [31] J.A.M. Ferreira, M.A.P. Amaral, F. V Antunes, J.D.M. Costa, A study on the mechanical behaviour of WC / Co hardmetals, (2008) 1–8. doi:10.1016/j.ijrmhm.2008.01.013.
- [32] J. Heinrichs, M. Olsson, I.Z. Jenei, S. Jacobson, Transfer of titanium in sliding contacts- New discoveries and insights revealed by in situ studies in the SEM, *Wear.* 315 (2014) 87–94. doi:10.1016/j.wear.2014.04.006.
- [33] L. Jin, A. Edrissy, A. R. Riahi, Analysis of Ti–6Al–4V adhesion to AISI 52100 steel and TiN during unlubricated sliding contact, *Tribol. Int.* 90 (2015) 278–286. doi:10.1016/j.triboint.2015.04.026.
- [34] A.F. Yetim, A. Celik, A. Alsaran, Improving tribological properties of Ti6Al4V alloy with duplex surface treatment, *Surf. Coatings Technol.* 205 (2010) 320–324. doi:10.1016/j.surfcoat.2010.06.048

APPENDIX A – PICTURES OF SCRATCH TEST RESULTS

Scratch tests were conducted with loading of 10N – 50N at loading increment of 10 N/mm, therefore the scratches has 4 mm length.

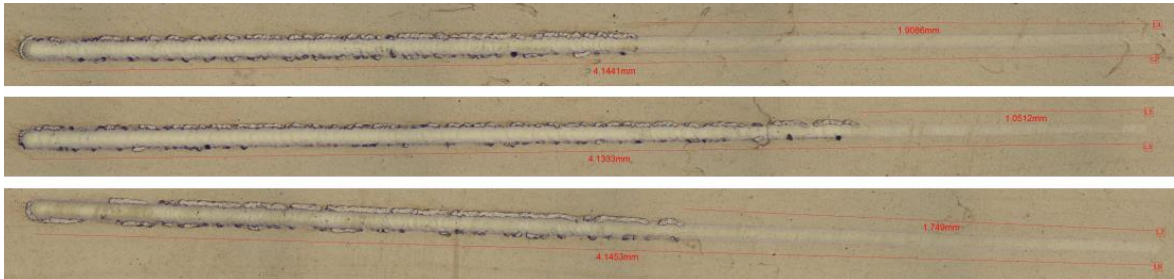


Figure A.1. Scratches of WTiN

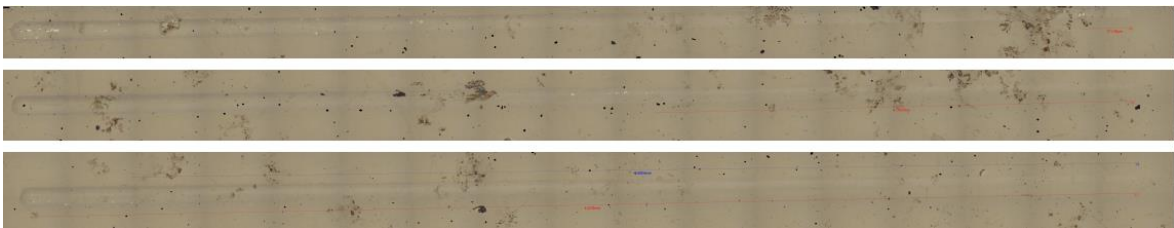


Figure A.2. Scratches of TiSiVN #1



Figure A.3. Scratches of TiSiVN #2

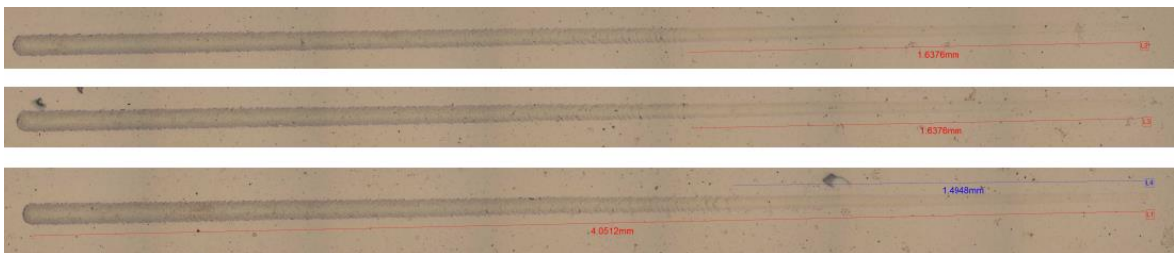


Figure A.4. Scratches of TiSiVN #3

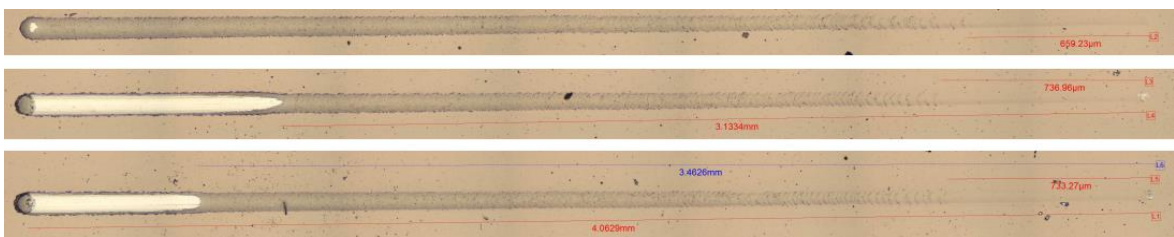


Figure A.5. Scratches of TiSiVN #4

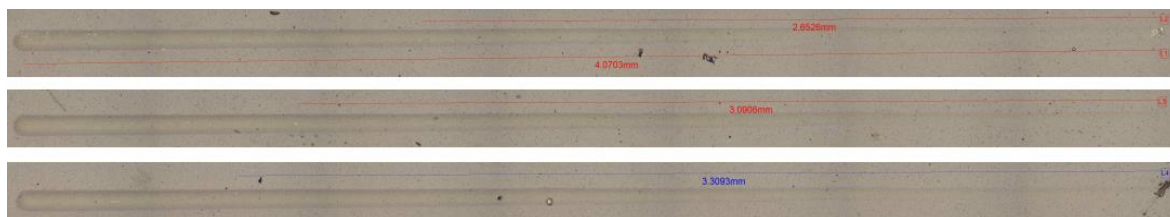


Figure A.6. Scratches of TiSiVN #5



Figure A.7. Scratches of TiSiVN #6

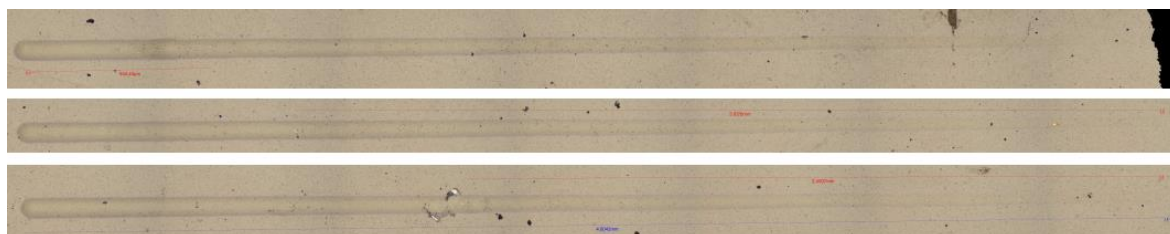


Figure A.8. Scratches of TiSiVN #7



Figure A.9. Scratches of TiSiVN #8

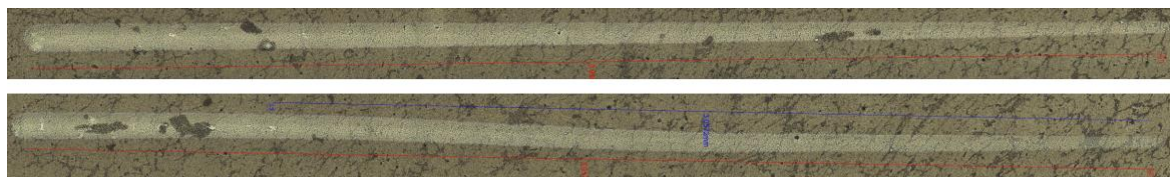


Figure A.10. Scratches of TEandM #2

APPENDIX B – 3D PROFILES OF BALLS WEAR SCARS

Three dimensional profiles were acquired with Alicona InfiniteFocus light microscope. The corresponding fresh/virgin surface of the tested ball served as the reference to measure the volume of scar profiles (volume above and below the references). The linear distance in dry tests were 20 μm and in lubricated test 100 μm . Normal load and linear speed were the same in all conditions: 5 N and 0.1 m/s, respectively.

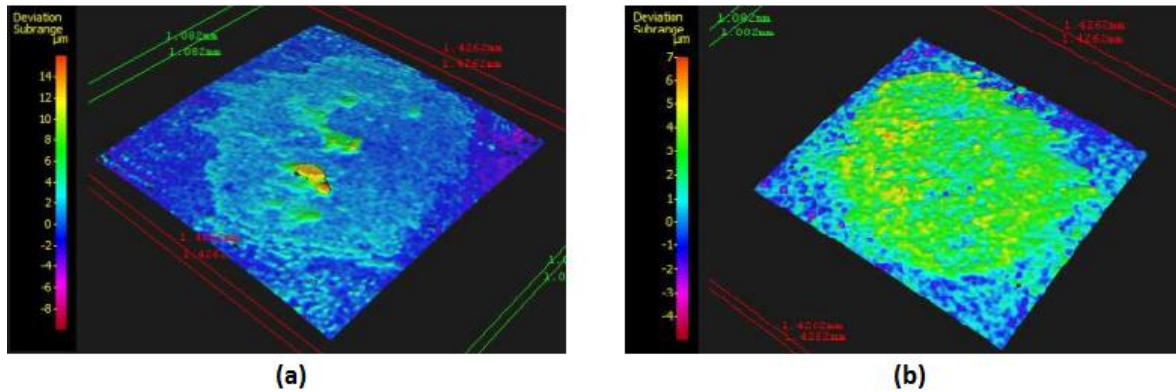


Figure B.1. Wear scar on uncoated ball: (a) dry test; (b) lubricated test

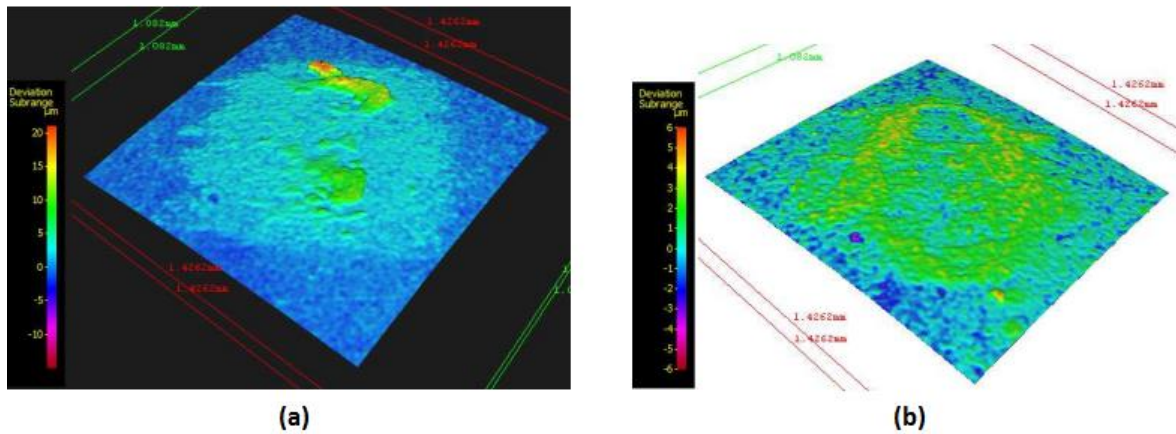


Figure B.2. Wear scar on WTiN ball: (a) dry test; (b) lubricated test

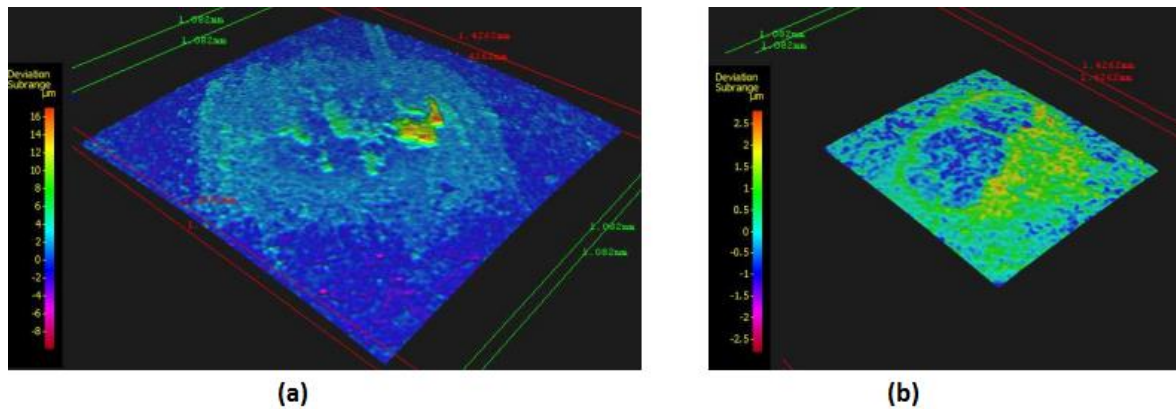


Figure B.3. Wear scar on TiSiVN #1 ball: (a) dry test; (b) lubricated test

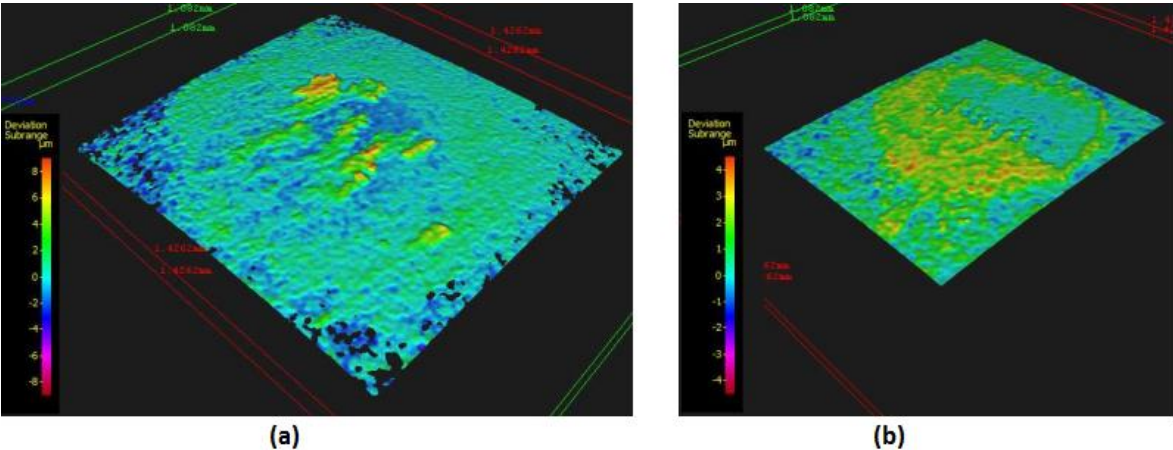


Figure B.4. Wear scar on TiSiVN #2 ball: (a) dry test; (b) lubricated test

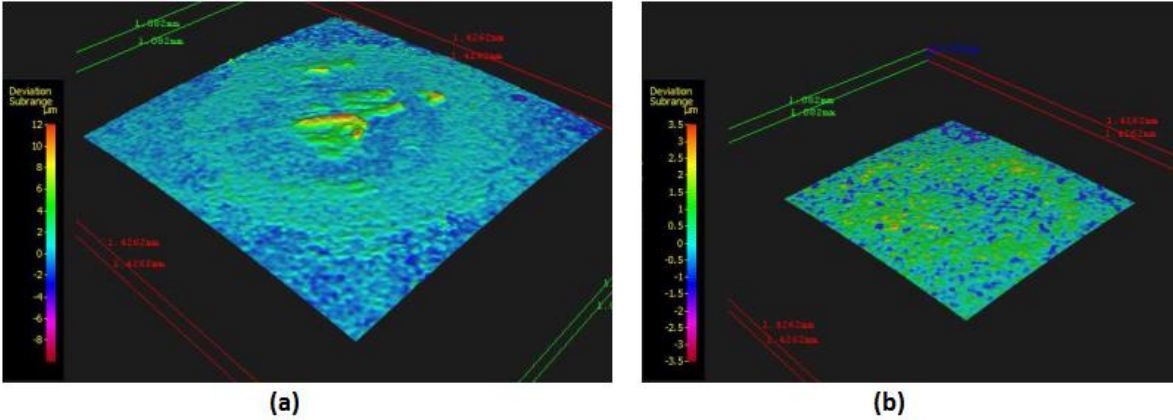


Figure B.5. Wear scar on TiSiVN #3 ball: (a) dry test; (b) lubricated test

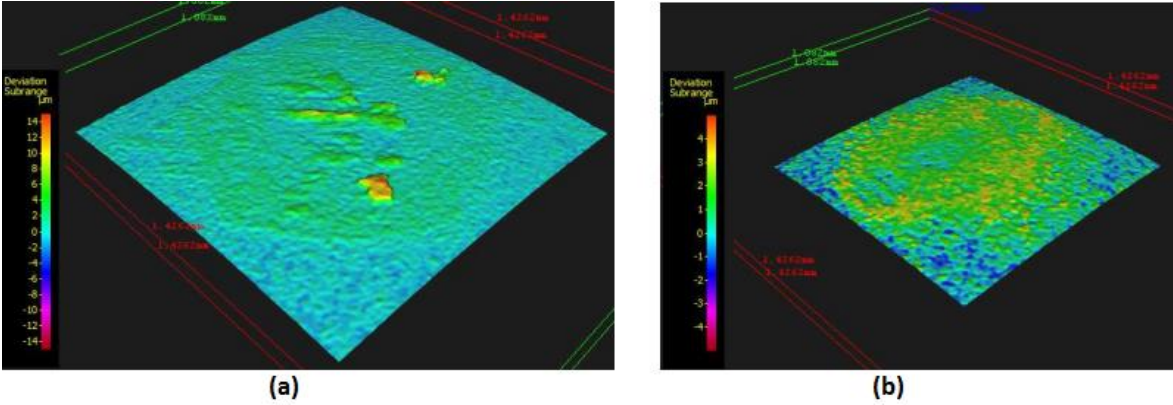


Figure B.6. Wear scar on TiSiVN #4 ball: (a) dry test; (b) lubricated test

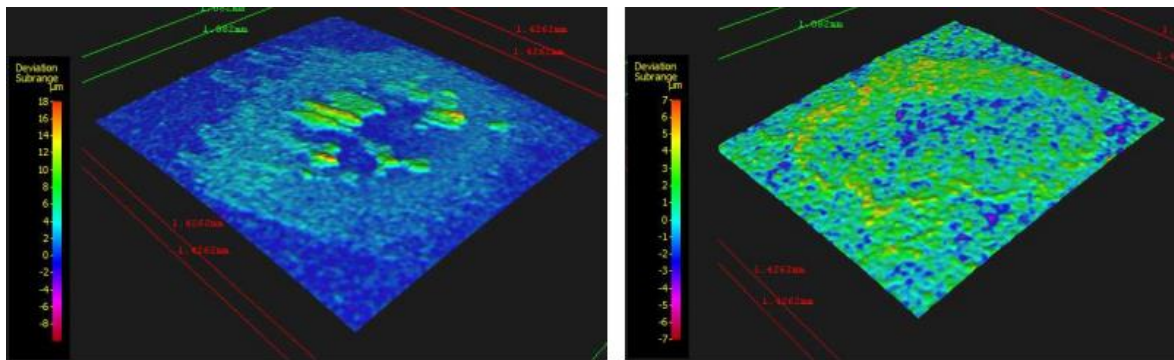


Figure B.7. Wear scar on TiSiVN #5 ball: (a) dry test; (b) lubricated test

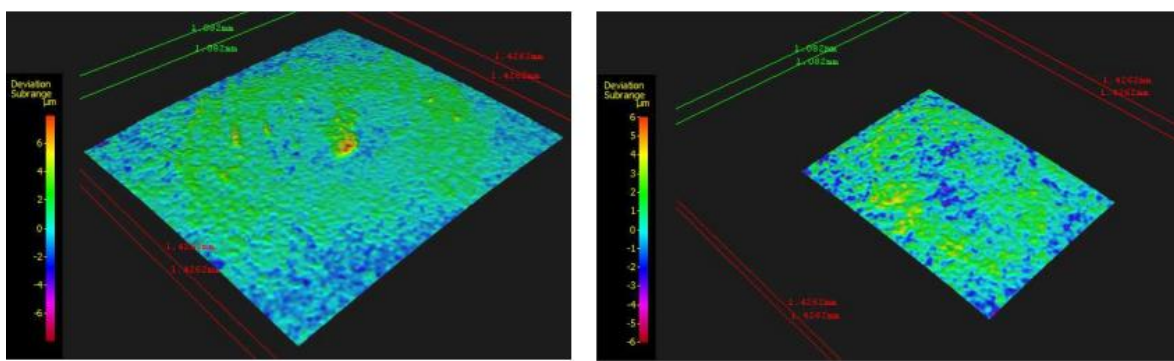


Figure B.8. Wear scar on TiSiVN #6 ball: (a) dry test; (b) lubricated test

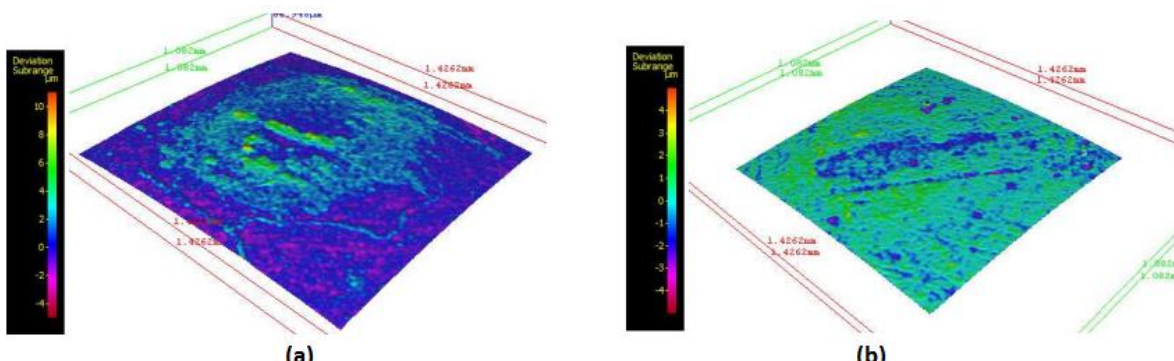


Figure B.9. Wear scar on TiSiVN #7 ball: (a) dry test; (b) lubricated test

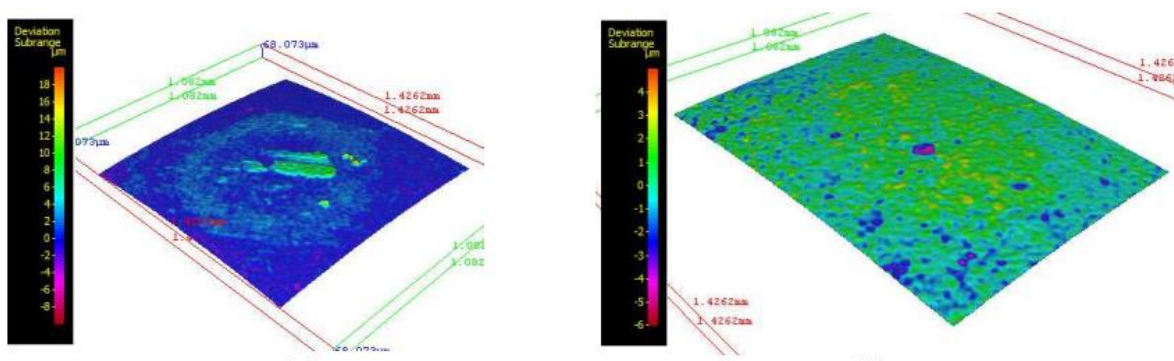


Figure B.10. Wear scar on TiSiVN #8 ball: (a) dry test; (b) lubricated test

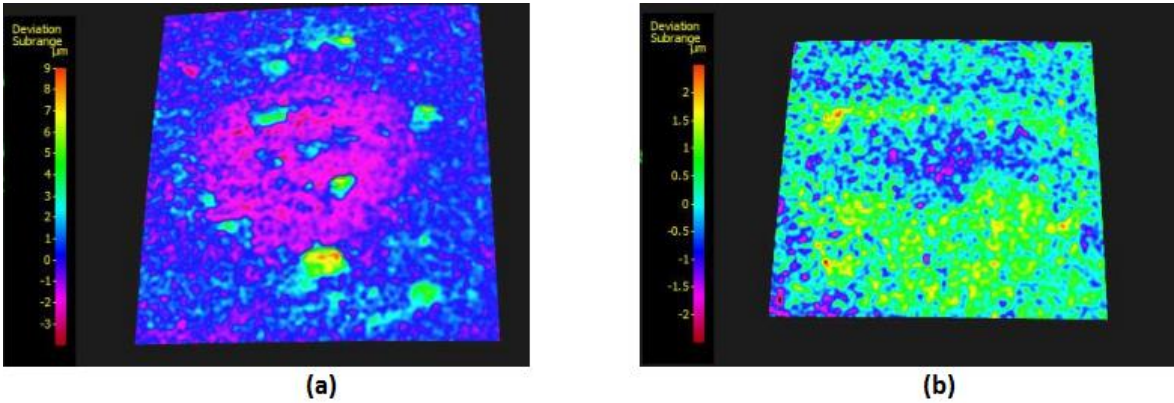


Figure B.11. Wear scar on TEandM #2 ball: (a) dry test; (b) lubricated test

APPENDIX C – RUNNING-IN PERIOD OF FRICTION COEFFICIENT

These figures show the early part of friction coefficient evolution over distance, to enable observation on the behaviour of samples during running-in period. The range for dry and lubricated conditions are the first 5 m and 10 m, respectively.

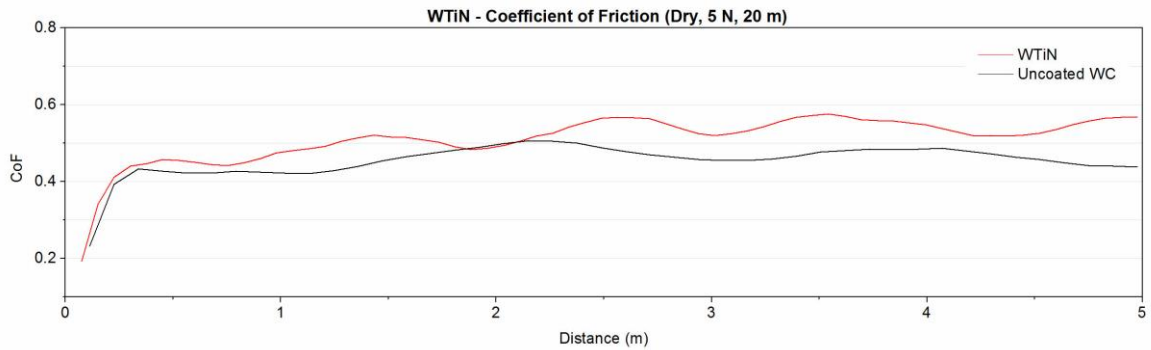


Figure C.1. Running in period of WTiN in dry condition

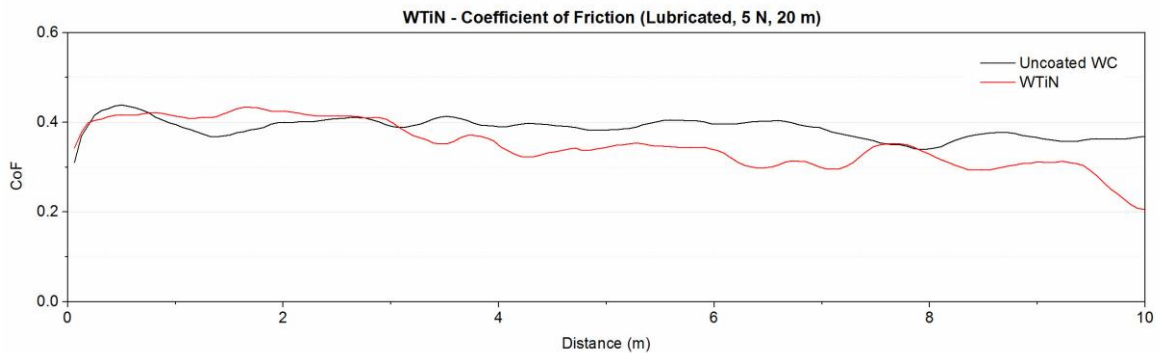


Figure C.2. Running in period of WTiN in lubricated condition

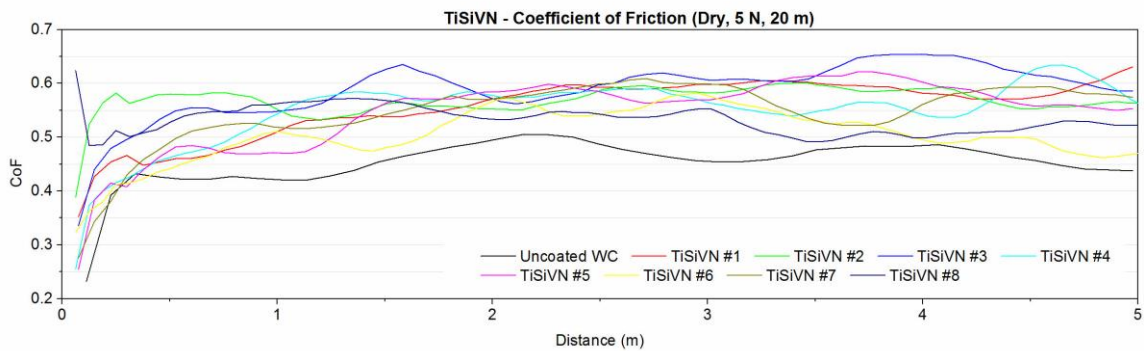


Figure C.3. Running in period of TiSiVN in dry condition

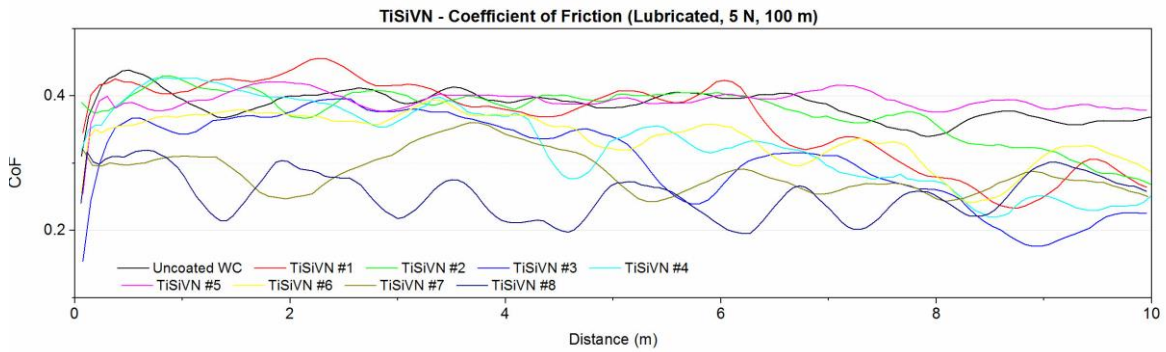


Figure C.4. Running in period of TiSiVN in lubricated condition

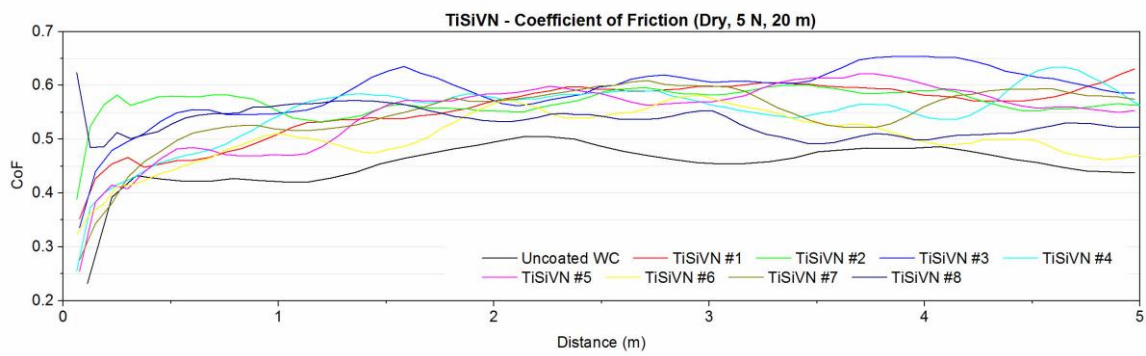


Figure C.5. Running in period of TEandM coatings in dry condition

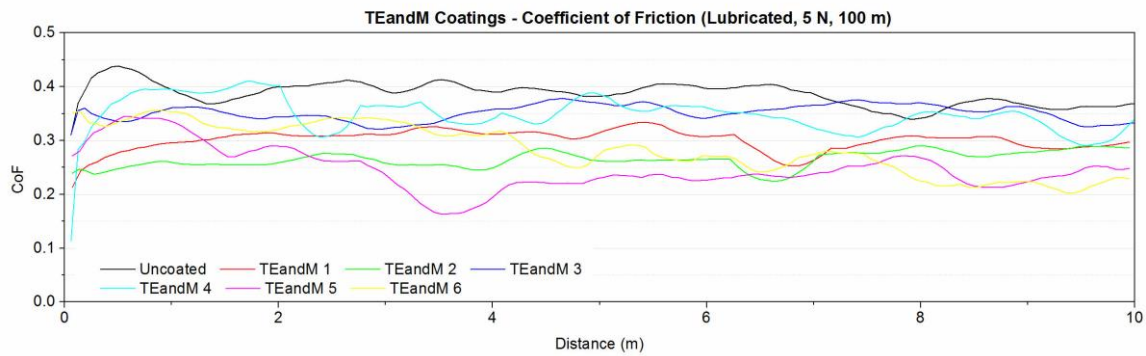


Figure C.6. Running in period of TEandM coatings in lubricated condition